Nonclassicality and entanglement criteria for bipartite optical fields characterized by quadratic detectors

Jan Peřina, Jr.,[*] and Ievgen I. Arkhipov
RCPTM, Joint Laboratory of Optics of Palacký University and Institute of Physics of the Czech Academy of Sciences, Faculty of Science, Palacký University, 17. listopadu 12, 77146 Olomouc, Czech Republic

Václav Michálek and Ondřej Haderka
Institute of Physics of the Czech Academy of Sciences, Joint Laboratory of Optics of Palacký University and Institute of Physics of CAS, 17. listopadu 50a, 77207 Olomouc, Czech Republic

(Received 23 May 2017; published 18 October 2017)

Numerous inequalities involving moments of integrated intensities and revealing nonclassicality and entanglement in bipartite optical fields are derived using the majorization theory, nonnegative polynomials, the matrix approach, and the Cauchy-Schwarz inequality. Different approaches for deriving these inequalities are compared. Using the experimental photocount histogram generated by a weak noisy twin beam monitored by a photon-number-resolving intensified CCD camera, the performance of the derived inequalities is compared. A basic set of 10 inequalities suitable for monitoring entanglement of a twin beam is suggested. Inequalities involving moments of photocounts (photon numbers) as well as some containing directly the elements of photocount (photon-number) distributions are also discussed as a tool for revealing nonclassicality.

DOI: 10.1103/PhysRevA.96.043845

I. INTRODUCTION

The notion of a nonclassical field was rigorously defined once the famous Glauber-Sudarshan representation of the density matrix of an optical field was formulated [1,2]. Since that time, any optical field with a nonpositive Glauber-Sudarshan quasidistribution has been considered nonclassical [3–6]. Analysis of more complex optical fields involving several optical modes has shown that one of the reasons for a field's nonclassicality is the presence of quantum correlations (entanglement) among the modes that constitute the field. As entanglement is interesting both for fundamental reasons and for various applications (in metrology, quantum-key distribution, etc.), it has been extensively studied in numerous publications in the last 10 years. The simplest case of entanglement between two fields has naturally attracted the greatest attention. In this case, even the quantification of entanglement has been found using the Schmidt number for pure states [7] and its generalization to mixed states based on finding the closest pure entangled state. Also, an alternative quantification derived from the shape of the Wigner function has been given [8]. Unfortunately, these theoretical approaches are difficult to apply to experimental optical fields [9,10]. From the experimental point of view, joint homodyne tomography [11,12] of both fields is needed to reveal the joint phase-space quasidistribution of these fields and, subsequently, quantify the entanglement via the mentioned theoretical approaches.

The great experimental demands of entanglement quantification lead to the simpler concept of entanglement witnesses (criteria) when dealing with entanglement. An entanglement witness is a physical quantity which identifies entanglement qualitatively through its values. Typically, this quantity is constructed from an inequality fulfilled by any classical optical field. The well-known and frequently used positive partial transpose (PPT) criterion [13,14] represents an entanglement witness that exploits the eigenvalues of a certain matrix. For specific systems, this witness can even be converted into an entanglement measure called the negativity [15]. There exists in principle an infinite number of entanglement witnesses. On the other hand, some of these witnesses are more important (or useful) for physical reasons. These reasons are pragmatic and they are related to the witnesses' performance in the experimental characterization of optical fields. As quadratic optical detectors are by far the most frequently used detectors in optical laboratories worldwide, witnesses exploiting the moments of integrated intensity (henceforth, just intensity) are extraordinarily important [16–20]. We note that the measurement of the whole joint photocount distribution of a bipartite optical field can be used to reconstruct the joint quasidistribution of integrated intensities [3,16,21] and to reveal its negative values observed for nonclassical states.

Here, we theoretically as well as experimentally analyze the witnesses that indicate negative values of the Glauber-Sudarshan quasidistribution of intensities. When applied to the whole optical field they represent global nonclassicality criteria (GNCCa). On the other hand, they serve as local nonclassicality criteria (LNCCa) in cases of marginal fields describing individual optical modes. For bipartite optical fields with classical constituents, the GNCCa represent also entanglement witnesses (criteria). The reason is that the global nonclassicality in general reflects either local nonclassicalities of the constituents, or entanglement between the constituents, or both. Twin beams with their signal and idler beams containing many photon pairs represent a typical example of such bipartite optical fields. The GNCCa and LNCCa are derived by several approaches that use the majorization theory [22], consider nonnegative polynomials and quadratic forms (the matrix approach) [23,24], and exploit the Cauchy-Schwarz inequality. Relying on the Mandel photodetection formula [3,4] the corresponding inequalities among the elements of the joint photocount and photon-number distributions are also

[*]jan.perina.jr@upol.cz

revealed. The performance of the derived GNCCa is tested on the experimental data characterizing a twin beam with around nine photon pairs on average and acquired by an intensified CCD (iCCD) camera. In this case, the GNCCa are also entanglement criteria.

The paper is organized as follows. In Sec. II, we give the simplest inequalities among the intensity moments. More complex inequalities including multiple intensity moments are derived in Sec. III using different approaches. Inequalities using the elements of the joint photocount and photon-number distributions are discussed in Sec. IV, together with some useful inequalities containing photocount and photon-number moments. Section V is devoted to the application of the derived inequalities to an experimental noisy twin beam. Conclusions are drawn in Sec. VI. Additional inequalities for identifying nonclassicality, which are redundant of those given in the text, are summarized in the Appendix for completeness.

II. SIMPLE NONCLASSICALITY CRITERIA USING INTENSITY MOMENTS

We consider a bipartite optical field composed of, in general, two entangled fields, which we call the signal and idler fields and which have intensities W_s and W_i, respectively. The overall field is described by the joint signal-idler intensity quasidistribution $P_{si}(W_s,W_i)$ [25], which allows us to determine the normally ordered (intensity) moments [3] along the relation

$$\langle W_s^k W_i^l\rangle = \int_0^\infty dW_s \int_0^\infty dW_i\, W_s^k W_i^l P_{si}(W_s,W_i),\quad k,l=0,1,\ldots. \tag{1}$$

According to the majorization theory applied to polynomials written in two independent variables [22,26], these intensity moments fulfill certain classical inequalities. Their negation gives us the series of global nonclassicality criteria

$$\sum_{\{k,l\}}\langle W_s^k W_i^l\rangle < \sum_{\{k',l'\}}\langle W_s^{k'} W_i^{l'}\rangle, \tag{2}$$

where the summation is performed over all possible permutations of the indices and the indices k and l majorize the indices k' and l' ($\{k,l\}\succ\{k',l'\}$). We note that such GNCCa are obtained in the general form of the sum (and difference) of mean values.

To understand in detail the structure of these GNCCa, we explicitly write those containing the intensity moments up to the fifth order in the form that naturally arises in the majorization theory:

$$\langle W_s^2\rangle+\langle W_i^2\rangle < 2\langle W_sW_i\rangle, \tag{3}$$

$$\langle W_s^3\rangle+\langle W_i^3\rangle < \langle W_s^2W_i\rangle+\langle W_sW_i^2\rangle, \tag{4}$$

$$\langle W_s^4\rangle+\langle W_i^4\rangle < \langle W_s^3W_i\rangle+\langle W_sW_i^3\rangle, \tag{5}$$

$$\langle W_s^4\rangle+\langle W_i^4\rangle < 2\langle W_s^2W_i^2\rangle, \tag{6}$$

$$\langle W_s^3W_i\rangle+\langle W_sW_i^3\rangle < 2\langle W_s^2W_i^2\rangle, \tag{7}$$

$$\langle W_s^5\rangle+\langle W_i^5\rangle < \langle W_s^4W_i\rangle+\langle W_sW_i^4\rangle, \tag{8}$$

$$\langle W_s^5\rangle+\langle W_i^5\rangle < \langle W_s^3W_i^2\rangle+\langle W_s^2W_i^3\rangle, \tag{9}$$

$$\langle W_s^4W_i\rangle+\langle W_sW_i^4\rangle < \langle W_s^3W_i^2\rangle+\langle W_s^2W_i^3\rangle. \tag{10}$$

However, the inequalities in Eqs. (3)–(10) can be recast, respectively, into the following:

$$\langle (W_s-W_i)^2\rangle < 0, \tag{11}$$

$$\langle (W_s+W_i)(W_s-W_i)^2\rangle < 0, \tag{12}$$

$$\langle (W_s^2+W_sW_i+W_i^2)(W_s-W_i)^2\rangle < 0, \tag{13}$$

$$\langle (W_s^2+2W_sW_i+W_i^2)(W_s-W_i)^2\rangle < 0, \tag{14}$$

$$\langle W_sW_i(W_s-W_i)^2\rangle < 0, \tag{15}$$

$$\langle (W_s+W_i)(W_s^2+W_i^2)(W_s-W_i)^2\rangle < 0, \tag{16}$$

$$\langle (W_s+W_i)(W_s^2+W_sW_i+W_i^2)(W_s-W_i)^2\rangle < 0, \tag{17}$$

$$\langle (W_s+W_i)W_sW_i(W_s-W_i)^2\rangle < 0. \tag{18}$$

A common property of these inequalities is that they are symmetric with respect to the exchange of indices s and i. This has its origin in the majorization theory.

The natural generalization of the above GNCCa that removes this symmetry and that is based upon mean values of nonnegative polynomials is written in the form of the following global nonclassicality criteria:

$$\langle W_s^kW_i^l(W_s-W_i)^{2m}\rangle < 0,\quad k,l=0,1,\ldots,\quad m=1,2\ldots. \tag{19}$$

Considering $m=1$ in Eq. (19) and intensity moments up to the fifth order, we may define the following GNCCa E:

$$E_{001}\equiv\langle W_s^2\rangle+\langle W_i^2\rangle-2\langle W_sW_i\rangle < 0, \tag{20}$$

$$E_{101}\equiv\langle W_s^3\rangle+\langle W_sW_i^2\rangle-2\langle W_s^2W_i\rangle < 0, \tag{21}$$

$$E_{011}\equiv\langle W_i^3\rangle+\langle W_s^2W_i\rangle-2\langle W_sW_i^2\rangle < 0, \tag{22}$$

$$E_{201}\equiv\langle W_s^4\rangle+\langle W_s^2W_i^2\rangle-2\langle W_s^3W_i\rangle < 0, \tag{23}$$

$$E_{021}\equiv\langle W_i^4\rangle+\langle W_s^2W_i^2\rangle-2\langle W_sW_i^3\rangle < 0, \tag{24}$$

$$E_{111}\equiv\langle W_s^3W_i\rangle+\langle W_sW_i^3\rangle-2\langle W_s^2W_i^2\rangle < 0, \tag{25}$$

$$E_{301}\equiv\langle W_s^5\rangle+\langle W_s^3W_i^2\rangle-2\langle W_s^4W_i\rangle < 0, \tag{26}$$

$$E_{031}\equiv\langle W_i^5\rangle+\langle W_s^2W_i^3\rangle-2\langle W_sW_i^4\rangle < 0, \tag{27}$$

$$E_{211}\equiv\langle W_s^4W_i\rangle+\langle W_s^2W_i^3\rangle-2\langle W_s^3W_i^2\rangle < 0, \tag{28}$$

$$E_{121}\equiv\langle W_sW_i^4\rangle+\langle W_s^3W_i^2\rangle-2\langle W_s^2W_i^3\rangle < 0. \tag{29}$$

The original GNCCa given in Eqs. (3)–(10) represent a subset of the GNCCa reported in Eqs. (20)–(29). In detail, the GNCCa in Eqs. (3)–(10) are expressed, respectively, as E_{001}, $E_{101}+E_{011}$, $E_{201}+E_{111}+E_{021}$, $E_{201}+2E_{111}+E_{021}$, E_{111}, $E_{301}+E_{211}+E_{121}+E_{031}$, $E_{301}+2E_{211}+2E_{121}+E_{031}$, and $E_{211}+E_{121}$.

Moreover, the consideration of $m=2$ in Eq. (19) gives us an additional three GNCCa:

$$E_{002}\equiv\langle W_s^4\rangle-4\langle W_s^3W_i\rangle+6\langle W_s^2W_i^2\rangle-4\langle W_sW_i^3\rangle+\langle W_i^4\rangle < 0, \tag{30}$$

$$E_{102} \equiv \langle W_s^5\rangle - 4\langle W_s^4 W_i\rangle + 6\langle W_s^3 W_i^2\rangle - 4\langle W_s^2 W_i^3\rangle + \langle W_s W_i^4\rangle < 0, \quad (31)$$

$$E_{012} \equiv \langle W_s^4 W_i\rangle - 4\langle W_s^3 W_i^2\rangle + 6\langle W_s^2 W_i^3\rangle - 4\langle W_s W_i^4\rangle + \langle W_i^5\rangle < 0. \quad (32)$$

These GNCCa can be expressed as linear combinations of some of the GNCCa written in Eqs. (20)–(29):

$$E_{002} = E_{201} + E_{021} - 2E_{111},$$
$$E_{102} = E_{301} + E_{121} - 2E_{211},$$
$$E_{012} = E_{211} + E_{031} - 2E_{121}. \quad (33)$$

As negative signs occur in the combinations of GNCCa E on the right-hand sides of Eqs. (33), the GNCCa E_{002}, E_{102}, and E_{012} are nontrivial and enrich the set of GNCCa given in Eqs. (20)–(29). We note that an analogous situation is met for $m > 2$ in Eq. (19) and higher-order intensity moments.

III. NONCLASSICALITY CRITERIA CONTAINING MULTIPLE INTENSITY MOMENTS

In this section, we derive the nonclassicality criteria that involve products of intensity moments. We concentrate our attention on the GNCCa containing products of two intensity moments, though several GNCCa encompassing also products of three intensity moments are mentioned. To determine these GNCCa we first apply the majorization theory. Then we exploit nonnegative polynomials to arrive at additional GNCCa. For completeness, we mention the GNCCa reached by the matrix approach, which uses nonnegative quadratic forms, and those derived from the Cauchy-Schwarz inequality. In parallel, we also reveal LNCCa containing intensity moments and provided by the majorization theory.

A. Nonclassicality criteria based on the majorization theory

We use again the formulas of the majorization theory [22], now in a systematic way. We begin with the majorization theory applied to polynomials written in two independent variables, W_s and W_i. Contrary to the approach in the previous section, we carry out averaging with the factorized quasidistribution function $P_s(W_s)P_i(W_i)$, where P_s (P_i) stands for the signal (idler) reduced quasidistribution function. The original Eq. (2) attains in this case the form of the local nonclassicality criteria,

$$\sum_{\{k,l\}} \langle W_s^k\rangle\langle W_i^l\rangle < \sum_{\{k',l'\}} \langle W_s^{k'}\rangle\langle W_i^{l'}\rangle, \quad (34)$$

with $\{k,l\} \succ \{k',l'\}$. Considering intensity moments up to the fifth order, we arrive at the following six LNCCa expressed in terms of the intensity moments of the local signal and idler fields:

$$B_{11}^{20} \equiv \langle W_s^2\rangle + \langle W_i^2\rangle - 2\langle W_s\rangle\langle W_i\rangle < 0, \quad (35)$$

$$B_{21}^{30} \equiv \langle W_s^3\rangle + \langle W_i^3\rangle - \langle W_s^2\rangle\langle W_i\rangle - \langle W_s\rangle\langle W_i^2\rangle < 0, \quad (36)$$

$$B_{31}^{40} \equiv \langle W_s^4\rangle + \langle W_i^4\rangle - \langle W_s^3\rangle\langle W_i\rangle - \langle W_s\rangle\langle W_i^3\rangle < 0, \quad (37)$$

$$B_{22}^{31} \equiv \langle W_s^3\rangle\langle W_i\rangle + \langle W_s\rangle\langle W_i^3\rangle - 2\langle W_s^2\rangle\langle W_i^2\rangle < 0, \quad (38)$$

$$B_{41}^{50} \equiv \langle W_s^5\rangle + \langle W_i^5\rangle - \langle W_s^4\rangle\langle W_i\rangle - \langle W_s\rangle\langle W_i^4\rangle < 0, \quad (39)$$

$$B_{32}^{41} \equiv \langle W_s^4\rangle\langle W_i\rangle + \langle W_s\rangle\langle W_i^4\rangle - \langle W_s^3\rangle\langle W_i^2\rangle - \langle W_s^2\rangle\langle W_i^3\rangle < 0. \quad (40)$$

The above LNCCa can be completed with simpler criteria that have their origin in the majorization theory applied to polynomials written in two independent variables, W_a and W_a', which uses averaging with the quasidistribution function $P_a(W_a)P_a(W_a')$, $a =$ s,i. These local nonclassicality criteria are obtained in the form [27–30]:

$$^aL_{11}^{20} \equiv \langle W_a^2\rangle - \langle W_a\rangle^2 < 0, \quad (41)$$

$$^aL_{21}^{30} \equiv \langle W_a^3\rangle - \langle W_a^2\rangle\langle W_a\rangle < 0, \quad (42)$$

$$^aL_{31}^{40} \equiv \langle W_a^4\rangle - \langle W_a^3\rangle\langle W_a\rangle < 0, \quad (43)$$

$$^aL_{22}^{31} \equiv \langle W_a^3\rangle\langle W_a\rangle - \langle W_a^2\rangle^2 < 0, \quad (44)$$

$$^aL_{41}^{50} \equiv \langle W_a^5\rangle - \langle W_a^4\rangle\langle W_a\rangle < 0, \quad (45)$$

$$^aL_{32}^{41} \equiv \langle W_a^4\rangle\langle W_a\rangle - \langle W_a^3\rangle\langle W_a^2\rangle < 0. \quad (46)$$

We note that the LNCCa given in Eqs. (35)–(46) occur in more complex expressions derived below, which combine the local nonclassicalities with the entanglement. We also note that the simplest LNCC given in Eq. (41) was experimentally observed already in 1977 using the light from fluorescence of a single molecule [31].

To reveal more complex GNCCa, we first analyze the formulas of the majorization theory with three independent variables, W_s, W_i, and W_a', considering two kinds of averaging with the quasidistribution functions $P_{si}(W_s,W_i)P_a(W_a')$, $a =$ s,i. To demonstrate the structure of the obtained inequalities without treating more complex formulas, we investigate the inequalities including intensity moments up to the fourth order. Detailed analysis of the majorization formulas denoted in standard notation $\{200\} \succ \{110\}$, $\{300\} \succ \{210\}$, $\{400\} \succ \{310\}$, and $\{310\} \succ \{220\}$ reveals that all these inequalities are obtained as suitable positive linear combinations of some of the inequalities written in Eqs. (20)–(29) and (35)–(46) and so they are redundant for the indication of nonclassicality. They can be found in the Appendix [Eqs. (A17)–(A20)]. The remaining majorization inequalities, $\{210\} \succ \{111\}$ and $\{220\} \succ \{211\}$, considered with both types of averaging, then provide the following four global nonclassicality criteria ($a =$ s,i):

$$^aD_{111}^{210} \equiv 2\langle W_a^2\rangle\langle W_a\rangle + \langle W_s^2 W_i\rangle + \langle W_s W_i^2\rangle + \langle W_s^2\rangle\langle W_i\rangle + \langle W_s\rangle\langle W_i^2\rangle - 6\langle W_a\rangle\langle W_s W_i\rangle < 0, \quad (47)$$

$$^aD_{211}^{220} \equiv \langle W_a^2\rangle^2 + \langle W_s^2 W_i^2\rangle + \langle W_s^2\rangle\langle W_i^2\rangle - \langle W_a\rangle \times \left[\langle W_s^2 W_i\rangle + \langle W_s W_i^2\rangle\right] - \langle W_a^2\rangle\langle W_s W_i\rangle < 0. \quad (48)$$

In the next step, we analyze the majorization inequalities with four independent variables, W_s, W_i, W_s', and W_i', and we use the quasidistribution function $P_{si}(W_s,W_i)P_{si}(W_s',W_i')$ for averaging. The inequalities $\{2000\} \succ \{1100\}$, $\{3000\} \succ \{2100\}$, $\{4000\} \succ \{3100\}$, and $\{3100\} \succ \{2200\}$ can be expressed as positive linear combinations of those given in

Eqs.(20)–(29) and (35)–(46), and as such they are not interesting for revealing nonclassicality. Similarly, the doubled inequality $\{2100\} \succ \{1110\}$ [$\{2200\} \succ \{2110\}$] is obtained as the sum ${}^{\rm s}D_{111}^{210} + {}^{\rm i}D_{111}^{210}$ [${}^{\rm s}D_{211}^{220} + {}^{\rm i}D_{211}^{220}$] of the GNCCa written in Eq. (47) [(48)]. More details are given in the Appendix [see Eqs. (A21)–(A26)]. Only the inequality $\{2110\} \succ \{1111\}$ is recast into the following global nonclassicality criterion:

$$D_{1111}^{2110} \equiv [\langle W_{\rm s}^2 W_{\rm i}\rangle + \langle W_{\rm s} W_{\rm i}^2\rangle][\langle W_{\rm s}\rangle + \langle W_{\rm i}\rangle] + \langle W_{\rm s} W_{\rm i}\rangle \times [\langle W_{\rm s}^2\rangle + \langle W_{\rm i}^2\rangle] - 6\langle W_{\rm s} W_{\rm i}\rangle^2 < 0. \quad (49)$$

The remaining inequalities up to the fourth order are provided by the majorization inequalities $\{2100\} \succ \{1110\}$, $\{2200\} \succ \{2110\}$, and $\{2110\} \succ \{1111\}$ if we perform averaging with the three quasidistribution functions $P_{\rm si}(W_{\rm s},W_{\rm i})P_a(W_a')P_a(W_a'')$, $a = {\rm s,i}$, and $P_{\rm si}(W_{\rm s},W_{\rm i})P_{\rm s}(W_{\rm s}')P_{\rm i}(W_{\rm i}')$, respectively. The occurrence of three intensity moments in a product represents their common feature. Step by step, the corresponding global nonclassicality criteria are derived in the form ($a = {\rm s,i}$)

$${}^aT_{1110}^{2100} \equiv 6\langle W_a^2\rangle\langle W_a\rangle + \langle W_{\rm s}^2 W_{\rm i}\rangle + \langle W_{\rm s} W_{\rm i}^2\rangle + 2\langle W_{\rm s}^2\rangle\langle W_{\rm i}\rangle + 2\langle W_{\rm s}\rangle\langle W_{\rm i}^2\rangle - 6\langle W_a\rangle\langle W_{\rm s} W_{\rm i}\rangle - 3\langle W_a\rangle^2[\langle W_{\rm s}\rangle + \langle W_{\rm i}\rangle] < 0, \quad (50)$$

$$T_{1110}^{2100} \equiv 2\langle W_{\rm s}^2\rangle\langle W_{\rm s}\rangle + 2\langle W_{\rm i}^2\rangle\langle W_{\rm i}\rangle + \langle W_{\rm s}^2 W_{\rm i}\rangle + \langle W_{\rm s} W_{\rm i}^2\rangle + 3\langle W_{\rm s}^2\rangle\langle W_{\rm i}\rangle + 3\langle W_{\rm s}\rangle\langle W_{\rm i}^2\rangle - 3[\langle W_{\rm s}\rangle + \langle W_{\rm i}\rangle] \times \langle W_{\rm s} W_{\rm i}\rangle - 3\langle W_{\rm s}\rangle^2\langle W_{\rm i}\rangle - 3\langle W_{\rm s}\rangle\langle W_{\rm i}\rangle^2 < 0, \quad (51)$$

$${}^aT_{2110}^{2200} \equiv 6\langle W_a^2\rangle^2 + 2\langle W_{\rm s}^2 W_{\rm i}^2\rangle + 4\langle W_{\rm s}^2\rangle\langle W_{\rm i}^2\rangle - 2\langle W_a\rangle^2\langle W_a^2\rangle - \langle W_a\rangle^2[\langle W_{\rm s}^2\rangle + \langle W_{\rm i}^2\rangle] - 2\langle W_a\rangle[\langle W_{\rm s}^2 W_{\rm i}\rangle + \langle W_{\rm s} W_{\rm i}^2\rangle] - 2\langle W_a^2\rangle[\langle W_{\rm s} W_{\rm i}\rangle + \langle W_{\rm s}\rangle\langle W_{\rm i}\rangle] < 0, \quad (52)$$

$$T_{2110}^{2200} \equiv 2\langle W_{\rm s}^2\rangle^2 + 2\langle W_{\rm i}^2\rangle^2 + 2\langle W_{\rm s}^2 W_{\rm i}^2\rangle + 6\langle W_{\rm s}^2\rangle\langle W_{\rm i}^2\rangle - [\langle W_{\rm s}\rangle + \langle W_{\rm i}\rangle][\langle W_{\rm s}^2 W_{\rm i}\rangle + \langle W_{\rm s} W_{\rm i}^2\rangle] - [\langle W_{\rm s}^2\rangle + \langle W_{\rm i}^2\rangle][\langle W_{\rm s} W_{\rm i}\rangle + 2\langle W_{\rm s}\rangle\langle W_{\rm i}\rangle] - \langle W_{\rm s}^2\rangle\langle W_{\rm i}\rangle^2 - \langle W_{\rm s}\rangle^2\langle W_{\rm i}^2\rangle < 0, \quad (53)$$

$${}^aT_{1111}^{2110} \equiv 2\langle W_a^2\rangle\langle W_a\rangle^2 + 2\langle W_a\rangle[\langle W_{\rm s}^2 W_{\rm i}\rangle + \langle W_{\rm s} W_{\rm i}^2\rangle] + \langle W_a\rangle^2[\langle W_{\rm s}^2\rangle + \langle W_{\rm i}^2\rangle] + 2\langle W_a^2\rangle[\langle W_{\rm s} W_{\rm i}\rangle + \langle W_{\rm s}\rangle\langle W_{\rm i}\rangle] - 12\langle W_a\rangle^2\langle W_{\rm s} W_{\rm i}\rangle < 0, \quad (54)$$

$$T_{1111}^{2110} \equiv [\langle W_{\rm s}\rangle + \langle W_{\rm i}\rangle][\langle W_{\rm s}^2 W_{\rm i}\rangle + \langle W_{\rm s} W_{\rm i}^2\rangle] + [\langle W_{\rm s}^2\rangle + \langle W_{\rm i}^2\rangle][\langle W_{\rm s} W_{\rm i}\rangle + 2\langle W_{\rm s}\rangle\langle W_{\rm i}\rangle] + \langle W_{\rm s}^2\rangle\langle W_{\rm i}\rangle^2 + \langle W_{\rm s}\rangle^2\langle W_{\rm i}^2\rangle - 12\langle W_{\rm s}\rangle\langle W_{\rm i}\rangle\langle W_{\rm s} W_{\rm i}\rangle < 0. \quad (55)$$

We note that the approach leading to Eqs. (50)–(55) provides also additional redundant GNCCa, which are summarized in the Appendix [see Eqs. (A27)–(A34)].

Additional nonclassicality inequalities containing products of three intensity moments are reached from the majorization inequalities written for polynomials with three variables and assuming averaging with the factorized quasidistributions $P_{\rm s}(W_{\rm s})P_{\rm i}(W_{\rm i})P_a(W_a')$, $a = {\rm s,i}$. The majorization inequalities $\{210\} \succ \{111\}$ and $\{220\} \succ \{211\}$ leave us with the following local nonclassicality criteria in this case ($a = {\rm s,i}$):

$${}^aB_{111}^{210} \equiv \langle W_a^2\rangle\langle W_a\rangle + \langle W_{\rm s}^2\rangle\langle W_{\rm i}\rangle + \langle W_{\rm i}^2\rangle\langle W_{\rm s}\rangle - 3\langle W_a\rangle\langle W_{\rm s}\rangle\langle W_{\rm i}\rangle < 0, \quad (56)$$

$${}^aB_{211}^{220} \equiv \langle W_a^2\rangle^2 + 2\langle W_{\rm s}^2\rangle\langle W_{\rm i}^2\rangle + \langle W_a\rangle^2\langle W_a^2\rangle - \langle W_a\rangle^2 \times [\langle W_{\rm s}^2\rangle + \langle W_{\rm i}^2\rangle] - 2\langle W_a^2\rangle\langle W_{\rm s}\rangle\langle W_{\rm i}\rangle < 0. \quad (57)$$

Analyzing the inequalities originating in the majorization theory with intensity moments up to the fourth order, we finally arrive at those written among the terms with four intensity moments in the product. They are naturally derived from the majorization inequalities written for polynomials with four variables considering, in turn, the quasidistributions $P_{\rm s}(W_{\rm s})P_{\rm i}(W_{\rm i})P_a(W_a')P_a(W_a'')$, $a = {\rm s,i}$, and $P_{\rm s}(W_{\rm s})P_{\rm i}(W_{\rm i})P_{\rm s}(W_{\rm s}')P_{\rm i}(W_{\rm i}')$. In detail, the majorization inequality $\{2110\} \succ \{1111\}$ is recast considering the above averaging into the following local nonclassicality criteria ($a = {\rm s,i}$):

$${}^aB_{1111}^{2110} \equiv \langle W_a\rangle^2[\langle W_{\rm s}^2\rangle + \langle W_{\rm i}^2\rangle] + 2\langle W_a^2\rangle\langle W_{\rm s}\rangle\langle W_{\rm i}\rangle - 4\langle W_a\rangle^2\langle W_{\rm s}\rangle\langle W_{\rm i}\rangle < 0, \quad (58)$$

$$B_{1111}^{2110} \equiv \langle W_{\rm s}^2\rangle\langle W_{\rm i}\rangle^2 + \langle W_{\rm s}\rangle^2\langle W_{\rm i}^2\rangle + 2[\langle W_{\rm s}^2\rangle + \langle W_{\rm i}^2\rangle] \times \langle W_{\rm s}\rangle\langle W_{\rm i}\rangle - 6\langle W_{\rm s}\rangle^2\langle W_{\rm i}\rangle^2 < 0. \quad (59)$$

We note that also additional LNCCa arise from the majorization theory written for polynomials with three and four variables. However, they can be expressed as positive linear combinations of the above written LNCCa and so they are redundant. They are explicitly given in Eqs. (A1)–(A16) in the Appendix.

B. Nonclassicality criteria based on nonnegative polynomials

Similarly to the previous section, where we have used the mean values of nonnegative polynomials in Eq. (19), here we derive local and global nonclassicality criteria by negating the following classical inequalities:

$$\langle W_{\rm s}^k W_{\rm i}^l (W_{\rm s} - \langle W_{\rm s}\rangle)^{2m} (W_{\rm i} - \langle W_{\rm i}\rangle)^{2n}\rangle < 0, \quad k,l = 0,1,\ldots, \quad m,n = 0,1\ldots. \quad (60)$$

Concentrating on the signal field ($m = 1$ and $n = 0$) and restricting our attention to the LNCCa containing intensity moments up to the fifth order we recognize in Eqs. (60) the following LNCCa:

$$E_{0l10} \equiv \langle W_{\rm s}^2 W_{\rm i}^l\rangle + \langle W_{\rm s}\rangle^2\langle W_{\rm i}^l\rangle - 2\langle W_{\rm s}\rangle\langle W_{\rm s} W_{\rm i}^l\rangle < 0, \quad l = 1,2,3; \quad (61)$$

$$E_{1l10} \equiv \langle W_s^3 W_i^l \rangle + \langle W_s \rangle^2 \langle W_s W_i^l \rangle - 2\langle W_s \rangle \langle W_s^2 W_i^l \rangle < 0, \quad l = 1,2; \tag{62}$$

$$E_{2110} \equiv \langle W_s^4 W_i \rangle + \langle W_s \rangle^2 \langle W_s^2 W_i \rangle - 2\langle W_s \rangle \langle W_s^3 W_i \rangle < 0. \tag{63}$$

One additional LNCC (E_{0120}) and one additional GNCC (E_{1011}) are expressed as linear combinations of the LNCCa in Eqs. (61)–(63) with varying signs:

$$E_{0120} \equiv E_{2110} + \langle W_s \rangle^2 E_{0110} - 2\langle W_s \rangle E_{1110} < 0, \tag{64}$$

$$E_{1011} \equiv E_{1210} + \langle W_i \rangle^2 E_{1010} - 2\langle W_i \rangle E_{1110} < 0. \tag{65}$$

The LNCCa and GNCC given in Eqs. (61)–(65) with exchanged subscripts s and i provide additional LNCCa and GNCC that can be derived from the symmetry. Moreover, there exists another GNCC belonging to the fourth order and being symmetric with respect to subscripts s and i:

$$E_{0011} \equiv E_{0210} + \langle W_i \rangle^2 \, {}^{s}L_{11}^{20} - 2\langle W_i \rangle E_{0110} < 0. \tag{66}$$

We note that Eq. (60) considered for $l = n = 0$ also gives nontrivial LNCCa, which can be added to those written in Eqs. (41)–(46). They are expressed as

$$E_{1010} \equiv {}^{s}L_{21}^{30} - \langle W_s \rangle \, {}^{s}L_{11}^{20} < 0, \tag{67}$$

$$E_{2010} \equiv {}^{s}L_{31}^{40} - \langle W_s \rangle \, {}^{s}L_{21}^{30} < 0, \tag{68}$$

$$E_{3010} \equiv {}^{s}L_{41}^{50} - \langle W_s \rangle \, {}^{s}L_{31}^{40} < 0, \tag{69}$$

$$E_{0020} \equiv {}^{s}L_{31}^{40} - 3\langle W_s \rangle \, {}^{s}L_{21}^{30} + 3\langle W_s \rangle^2 \, {}^{s}L_{11}^{20} < 0, \tag{70}$$

$$E_{1020} \equiv {}^{s}L_{41}^{50} - 3\langle W_s \rangle \, {}^{s}L_{31}^{40} + 3\langle W_s \rangle^2 \, {}^{s}L_{21}^{30} - \langle W_s \rangle^3 \, {}^{s}L_{11}^{20} < 0. \tag{71}$$

C. Global nonclassicality criteria based on the matrix approach

In this case, the GNCCa are based on considering classically positive semidefinite matrices of dimension $n \times n$ for $n = 2,3,\ldots$ that describe mean values of quadratic forms defined above the basis which includes different powers of the signal and idler intensities. This approach has been elaborated in general for both the amplitude and the intensity moments in Refs. [23,32–34], summarized in Ref. [24], and applied in Ref. [19]. The Bochner theorem has been used to arrive at even more general forms of these inequalities [35,36]. For $n = 2$ the global nonclassicality criteria are defined along the relation $(i,j,k,l \geqslant 0)$

$$M_{ijkl} \equiv \langle W_s^{2i} W_i^{2j} \rangle \langle W_s^{2k} W_i^{2l} \rangle - \langle W_s^{i+k} W_i^{j+l} \rangle^2 < 0. \tag{72}$$

Restricting our considerations to the GNCCa up to the fifth order in intensity moments, we reveal only the following two inequalities:

$$M_{1100} \equiv \langle W_s^2 W_i^2 \rangle - \langle W_s W_i \rangle^2 < 0, \tag{73}$$

$$M_{1001} \equiv \langle W_s^2 \rangle \langle W_i^2 \rangle - \langle W_s W_i \rangle^2 < 0. \tag{74}$$

For comparison, we write two GNCCa originating in the majorization inequalities $\{2200\} \succ \{1111\}$ and $\{4000\} \succ \{1111\}$ considered with averaging over the quasidistribution function $P_{si}(W_s, W_i) P_{si}(W_s', W_i')$:

$$D_{1111}^{2200} \equiv \left[\langle W_s^2 \rangle + \langle W_i^2 \rangle\right]^2 + 2\langle W_s^2 W_i^2 \rangle - 6\langle W_s W_i \rangle^2 < 0, \tag{75}$$

$$D_{1111}^{4000} \equiv \langle W_s^4 \rangle + \langle W_i^4 \rangle - 2\langle W_s W_i \rangle^2 < 0. \tag{76}$$

We note that the GNCCa D_{1111}^{2200} and D_{1111}^{4000} stem from the GNCCa written in Eqs. (47)–(49) and the LNCCa summarized in Eqs. (35)–(46).

Also, a 3×3 matrix built above the base vector $(1, W_s, W_i)$ results in one global nonclassicality criterion of the fourth order:

$$M_{001001} \equiv \langle W_s^2 \rangle \langle W_i^2 \rangle + 2\langle W_s W_i \rangle \langle W_s \rangle \langle W_i \rangle - \langle W_s W_i \rangle^2 - \langle W_s^2 \rangle \langle W_i \rangle^2 - \langle W_s \rangle^2 \langle W_i^2 \rangle < 0. \tag{77}$$

D. Global nonclassicality criteria derived from the Cauchy-Schwarz inequality

To reveal additional global nonclassicality criteria, we negate the Cauchy-Schwarz inequality:

$$\left[\int dW_s dW_i P_{si}(W_s, W_i) f(W_s, W_i) g(W_s, W_i)\right]^2 > \int dW_s dW_i P_{si}(W_s, W_i) f^2(W_s, W_i) \times \int dW_s dW_i P_{si}(W_s, W_i) g^2(W_s, W_i). \tag{78}$$

In Eq. (78), f and g denote arbitrary real functions and P_{si} stands for the joint quasidistribution of integrated intensities. Restricting ourselves up to the fifth power of intensities, we may in turn consider $f = 1$ together with $g = W_s W_i$, $f = \sqrt{W_s}$ together with $g = \sqrt{W_s} W_i$, $f = W_s$ together with $g = W_i$, and $f = W_s \sqrt{W_i}$ together with $g = \sqrt{W_i}$ to arrive at the following GNCCa:

$$C_{22}^{00} \equiv \langle W_s^2 W_i^2 \rangle - \langle W_s W_i \rangle^2 < 0, \tag{79}$$

$$C_{12}^{10} \equiv \langle W_s W_i^2 \rangle \langle W_s \rangle - \langle W_s W_i \rangle^2 < 0, \tag{80}$$

$$C_{02}^{20} \equiv \langle W_s^2 \rangle \langle W_i^2 \rangle - \langle W_s W_i \rangle^2 < 0, \tag{81}$$

$$C_{01}^{21} \equiv \langle W_s^2 W_i \rangle \langle W_i \rangle - \langle W_s W_i \rangle^2 < 0. \tag{82}$$

The criterion C_{22}^{00} in Eq. (79) [C_{02}^{20} in Eq. (81)] coincides with the criterion M_{1100} in Eq. (73) [M_{1001} in Eq. (74)] derived from the matrix approach.

All inequalities among the intensity moments discussed both in the previous and in this section can mutually be compared quantitatively when we transform these inequalities into the corresponding nonclassicality depths. In this approach, we replace the usual (normally ordered) intensity moments $\langle W^k \rangle$ with the moments $\langle W^k \rangle_s$ related to a general s ordering of the field operators according to the formula [3]

$$\langle W^k \rangle_s = \left(\frac{2}{1-s}\right)^k \left\langle \mathrm{L}_k\left(\frac{2W}{s-1}\right)\right\rangle, \tag{83}$$

in which L_k denotes the kth Laguerre polynomial [37]. Then we formally consider all the above inequalities originally derived for normally ordered intensity moments with s-ordered intensity moments and varying values of the parameter s. If a given inequality indicates nonclassicality for the normally ordered moments, decreasing values of the ordering parameter s gradually suppress this nonclassicality due to the increasing additional 'detection' noise [38]. The nonclassicality is lost for a certain threshold value $s_{\rm th}$. This value defines a nonclassicality depth (NCD) τ [38] as follows:

$$\tau = \frac{1 - s_{\rm th}}{2}. \tag{84}$$

The greater the value of the NCD τ is, the stronger the nonclassicality is.

IV. NONCLASSICALITY CRITERIA BASED ON THE ELEMENTS OF PHOTOCOUNT AND PHOTON-NUMBER DISTRIBUTIONS AND THEIR MOMENTS

All nonclassicality criteria based on intensity moments and thoroughly discussed in the previous two sections can be easily transformed into the corresponding criteria, which use the elements of the photon-number [photocount] distribution $p_{\rm si}(n_{\rm s},n_{\rm i})$ [$f_{\rm si}(c_{\rm s},c_{\rm i})$] [30,39–41]. To understand this, we first write the two-dimensional Mandel photodetection formula [3,4],

$$p_{\rm si}(n_{\rm s},n_{\rm i}) = \frac{1}{n_{\rm s}!\,n_{\rm i}!}\int_0^\infty dW_{\rm s}\int_0^\infty dW_{\rm i}\, W_{\rm s}^{n_{\rm s}} W_{\rm i}^{n_{\rm i}} \times \exp[-(W_{\rm s}+W_{\rm i})]P_{\rm si}(W_{\rm s},W_{\rm i}), \tag{85}$$

where $P_{\rm si}(W_{\rm s},W_{\rm i})$ is the above used joint quasidistribution of integrated intensities. Introducing the modified elements $\tilde{p}_{\rm si}$ of the photon-number distribution,

$$\tilde{p}_{\rm si}(n_{\rm s},n_{\rm i}) \equiv \frac{n_{\rm s}!\,n_{\rm i}!\,p_{\rm si}(n_{\rm s},n_{\rm i})}{p_{\rm si}(0,0)}, \tag{86}$$

and the properly normalized quasidistribution $\tilde{P}_{\rm si}$,

$$\tilde{P}_{\rm si}(W_{\rm s},W_{\rm i}) \equiv \exp[-(W_{\rm s}+W_{\rm i})]P_{\rm si}(W_{\rm s},W_{\rm i})\left[\int_0^\infty dW_{\rm s} \times \int_0^\infty dW_{\rm i}\exp[-(W_{\rm s}+W_{\rm i})]P_{\rm si}(W_{\rm s},W_{\rm i})\right]^{-1}, \tag{87}$$

the Mandel photodetection formula in Eq. (85) is recast in a form defining the modified elements $\tilde{p}_{\rm si}$ as the moments of the quasidistribution $\tilde{P}_{\rm si}$:

$$\tilde{p}_{\rm si}(n_{\rm s},n_{\rm i}) = \int_0^\infty dW_{\rm s}\int_0^\infty dW_{\rm i}\, W_{\rm s}^{n_{\rm s}} W_{\rm i}^{n_{\rm i}}\, \tilde{P}_{\rm si}(W_{\rm s},W_{\rm i}). \tag{88}$$

The formal substitution in the above derived nonclassicality criteria for intensity moments suggested by formula (88) is expressed as

$$\langle W_{\rm s}^{n_{\rm s}} W_{\rm i}^{n_{\rm i}}\rangle \longleftarrow \tilde{p}_{\rm si}(n_{\rm s},n_{\rm i}). \tag{89}$$

As an example, we rewrite the inequalities in Eq. (19) for $m=1$ into the following global nonclassicality criteria:

$$F_{kl1} \equiv \tilde{p}_{\rm si}(k+2,l) + \tilde{p}_{\rm si}(k,l+2) - 2\tilde{p}_{\rm si}(k+1,l+1) < 0, \quad k,l = 0,1,\ldots. \tag{90}$$

Alternatively, the inequalities for intensity moments can be directly transformed into the moments of photon numbers (photocounts) exploiting the relation between the 'factorial' photon-number moments (intensity moments) $\langle W^k\rangle$ and the usual photon-number moments $\langle n^k\rangle$. Using the Stirling numbers $S(k,l)$ of the second kind [28], its two-dimensional variant is expressed in the form

$$\langle n_{\rm s}^{k_{\rm s}} n_{\rm i}^{k_{\rm i}}\rangle = \sum_{l_{\rm s}=1}^{k_{\rm s}} S^{-1}(k_{\rm s},l_{\rm s}) \sum_{l_{\rm i}=1}^{k_{\rm i}} S^{-1}(k_{\rm i},l_{\rm i}) W_{\rm s}^{l_{\rm s}} W_{\rm i}^{l_{\rm i}}, \quad k_{\rm s},k_{\rm i} = 1,2,\ldots. \tag{91}$$

The Stirling numbers $S(k,l)$ of the second kind for the first five moments are conveniently expressed as a matrix S_{kl} that, together with its inverse matrix S_{kl}^{-1} giving the Stirling numbers of the first kind, takes the form

$$S_{kl} = \begin{bmatrix} 1 & 0 & 0 & 0 & 0 \\ 1 & 1 & 0 & 0 & 0 \\ 1 & 3 & 1 & 0 & 0 \\ 1 & 7 & 6 & 1 & 0 \\ 1 & 15 & 25 & 10 & 1 \end{bmatrix},$$

$$S_{kl}^{-1} = \begin{bmatrix} 1 & 0 & 0 & 0 & 0 \\ -1 & 1 & 0 & 0 & 0 \\ 2 & -3 & 1 & 0 & 0 \\ -6 & 11 & -6 & 1 & 0 \\ 24 & -50 & 35 & -10 & 1 \end{bmatrix}. \tag{92}$$

We note that the above formulas between the intensity and the photon-number moments assume an effective single-mode field. However, generalization to multimode fields may be considered, as has been done for multimode twin beams in Refs. [17] and [42]. Also, different LNCCa expressed in either the intensity or the photon-number moments have been compared in [30].

The linear relations between the photon-number moments and the intensity moments formulated in Eq. (91) can be used to rewrite the nonclassicality criteria from the previous two sections in terms of the photon-number moments. This is interesting, as the joint photocount distributions are directly experimentally accessible and the joint photon-number distributions are reached once we correct the experimental data for finite detection efficiencies [43]. The rewritten nonclassicality criteria, however, usually attain more complex forms compared to the original ones written for intensity moments. For this reason, we derive here only the nonclassicality criteria that involve cross-correlation moments containing different powers of the signal and idler photon numbers. They are obtained as suitable positive linear combinations of the GNCCa E written in Eqs. (20)–(29):

$$N_{11} \equiv E_{001} = \sum_{a={\rm s,i}} \left[\langle n_a^2\rangle - \langle n_a\rangle\right] - 2\langle n_{\rm s} n_{\rm i}\rangle < 0, \tag{93}$$

$$N_{21} \equiv E_{101} + E_{011} + E_{001} = \sum_{a={\rm s,i}} \left[\langle n_a^3\rangle - 2\langle n_a^2\rangle + \langle n_a\rangle\right] - \langle n_{\rm s}^2 n_{\rm i}\rangle - \langle n_{\rm s} n_{\rm i}^2\rangle < 0, \tag{94}$$

$$N_{31} \equiv E_{201} + E_{021} + E_{111} + 3(E_{101} + E_{011} + E_{001}) = \sum_{a=\mathrm{s,i}} [\langle n_a^4\rangle - 3\langle n_a^3\rangle + 5\langle n_a^2\rangle - 3\langle n_a\rangle] - 4\langle n_\mathrm{s} n_\mathrm{i}\rangle - \langle n_\mathrm{s}^3 n_\mathrm{i}\rangle - \langle n_\mathrm{s} n_\mathrm{i}^3\rangle < 0, \quad (95)$$

$$N_{22} \equiv E_{201} + E_{021} + 2E_{111} + 2(E_{101} + E_{011} + E_{001}) = \sum_{a=\mathrm{s,i}} [\langle n_a^4\rangle - 4\langle n_a^3\rangle + 7\langle n_a^2\rangle - 4\langle n_a\rangle] - 2\langle n_\mathrm{s} n_\mathrm{i}\rangle - 2\langle n_\mathrm{s}^2 n_\mathrm{i}^2\rangle < 0, \quad (96)$$

$$N_{41} \equiv E_{301} + E_{031} + E_{211} + E_{121} + 6(E_{201} + E_{021} + E_{111}) + 7(E_{101} + E_{011} + E_{001}) = \sum_{a=\mathrm{s,i}} [\langle n_a^5\rangle - 4\langle n_a^4\rangle + 6\langle n_a^3\rangle + 2\langle n_a^2\rangle - 5\langle n_a\rangle] - 12\langle n_\mathrm{s} n_\mathrm{i}\rangle - \langle n_\mathrm{s}^4 n_\mathrm{i}\rangle - \langle n_\mathrm{s} n_\mathrm{i}^4\rangle < 0, \quad (97)$$

$$N_{32} \equiv E_{301} + E_{031} + 2E_{211} + 2E_{121} + 4(E_{201} + E_{021}) + 7E_{111} + 4(E_{101} + E_{011}) + E_{001} = \sum_{a=\mathrm{s,i}} [\langle n_a^5\rangle - 6\langle n_a^4\rangle + 15\langle n_a^3\rangle - 17\langle n_a^2\rangle + 7\langle n_a\rangle] - \langle n_\mathrm{s}^3 n_\mathrm{i}^2\rangle - \langle n_\mathrm{s}^2 n_\mathrm{i}^3\rangle < 0. \quad (98)$$

V. EXPERIMENTAL VERIFICATION OF THE DERIVED NONCLASSICALITY AND ENTANGLEMENT CRITERIA

In order to experimentally judge the performance of the above derived nonclassicality criteria, we have applied them to the analysis of entanglement between the signal and the idler fields constituting a weak twin beam generated in the process of spontaneous parametric down-conversion [4,21]. The marginal signal and idler fields are generated with multimode thermal statistics which is a consequence of the spontaneous emission. As such the twin beam is locally classical and so the applied GNCCa are also the entanglement criteria. The twin beam was generated in a 5-mm-long type I barium-borate crystal (BaB_2O_4; BBO) cut to a slightly noncollinear geometry (for the experimental scheme, see Fig. 1). Parametric down-conversion was pumped by pulses originating in the third harmonics (280 nm) of a femtosecond cavity dumped Ti:sapphire laser that produced pulses with a duration of 150 fs and a central wavelength of 840 nm. The signal field as well as the idler field was detected in different strips of the photocathode of the iCCD camera (Andor DH334-18U-63). Before detection, the nearly-frequency-degenerate signal and idler photons at the wavelength of 560 nm were filtered with a 14-nm-wide bandpass interference filter. Moreover, to stabilize the pump intensity, and thus also the twin beam intensity, to minimize fluctuations in the measured photocount distribution, the pump beam was actively stabilized via a motorized half-wave plate followed by a polarizer and detector that monitored the actual intensity.

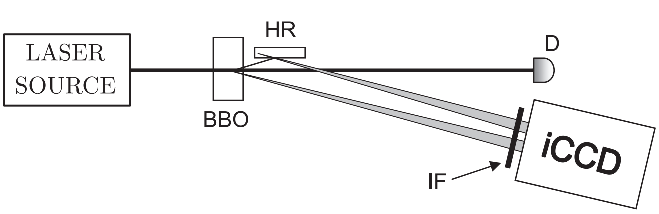

FIG. 1. Scheme of the experimental setup: A twin beam originating in a nonlinear crystal (BBO) pumped by an ultrashort pulse generates a weak twin beam. The signal field and the idler field (after reflection on the mirror; HR) are filtered with a bandpass interference filter (IF) and then detected by an iCCD camera. The pump-beam intensity is actively stabilized with feedback provided by the detector (D).

In the experiment, a joint signal-idler photocount histogram $f_\mathrm{si}(c_\mathrm{s},c_\mathrm{i})$ was determined, repeating the measurement 1.2×10^6 times. This histogram, obtained with a high precision due to the high number of repetitions, has allowed us to reconstruct the original joint signal-idler photon-number distribution $p_\mathrm{si}(n_\mathrm{s},n_\mathrm{i})$, which characterizes the twin beam before being detected. We have used two methods for the reconstruction. First, we have applied a method developed originally for detector calibration [44]. This method, in addition to giving the detection efficiencies η_s and η_i in the signal and idler fields, respectively, also gives the parameters of the twin beam used, though in the specific form of a multimode Gaussian field. Knowing the detection efficiencies as well as other parameters of the used iCCD camera, we have reconstructed the measured twin beam by the general approach of expectation maximization (maximum-likelihood approach) [45].

In the calibration method, the twin beam has been revealed in the analytical form of a multimode Gaussian field composed of independent multimode paired, noise signal and noise idler components characterized by mean photon(-pair) numbers B_a per mode and numbers M_a of independent modes, $a =$ p,s,i [21,25]. The corresponding photon-number distribution $p_\mathrm{si}(n_\mathrm{s},n_\mathrm{i})$ attains in this case the form of a twofold convolution among three Mandel-Rice photon-number distributions [3] belonging to the constituting paired, noise signal, and noise idler components [21,25,44]:

$$p_\mathrm{si}(n_\mathrm{s},n_\mathrm{i}) = \sum_{n=0}^{\min[n_\mathrm{s},n_\mathrm{i}]} p(n_\mathrm{s}-n; M_\mathrm{s}, B_\mathrm{s}) p(n_\mathrm{i}-n; M_\mathrm{i}, B_\mathrm{i}) \times p(n; M_\mathrm{p}, B_\mathrm{p}). \quad (99)$$

The Mandel-Rice distribution $p(n;M,B)$ is given as $p(n;M,B) = \Gamma(n+M)/[n!\,\Gamma(M)]B^n/(1+B)^{n+M}$ using the Γ function. Moreover, the response of the iCCD camera has to be described by an appropriate positive-operator-valued measure (POVM). For an iCCD camera with N_a active pixels, detection efficiency η_a, and mean dark count number per pixel D_a, this POVM, denoted $T_\mathrm{a}(c_\mathrm{a},n_\mathrm{a})$, has been derived in Ref. [43]:

$$T_a(c_a,n_a) = \binom{N_a}{c_a}(1-D_a)^{N_a}(1-\eta_a)^{n_a}(-1)^{c_a} \times \sum_{l=0}^{c_a} \binom{c_a}{l} \frac{(-1)^l}{(1-D_a)^l}\left(1 + \frac{l}{N_a}\frac{\eta_a}{1-\eta_a}\right)^{n_a}. \quad (100)$$

We note that the POVM $T_a(c_a,n_a)$ gives the probability of having c_a photocounts when detecting a field with n_a photons, $a = s,i$. With these premises, the method of the least squared declinations based on the distribution p_{si} in Eq. (99) and POVMs T_s and T_i for the signal and idler detection arms, respectively, gives both the detection efficiencies η_s and η_i and the parameters of the used twin beam. The calibration method applied to the experimental photocount histogram $f_{si}(c_s,c_i)$ gave us the parameter values $\eta_s = 0.230 \pm 0.005$, $\eta_i = 0.220 \pm 0.005$, $M_p = 270$, $B_p = 0.032$, $M_s = 0.01$, $B_s = 7.6$, $M_i = 0.026$, and $B_i = 5.3$ (relative experimental errors: 7%; for details, see [21]), in addition to those determined independently: $N_s = 6528$, $N_i = 6784$, and $D_s N_s = D_i N_i = 0.040 \pm 0.001$. We note that the distribution with a number M of modes considerably lower than 1 is highly peaked around the value $n = 0$, which is a consequence of the specific form of the noise occurring in the detection process. The obtained parameters reveal that the measured weak twin beam was composed of, on average, 8.8 photon pairs and 0.07 (0.15) noise signal (idler) photon. Its joint signal-idler photon-number distributions $p_{si}(n_s,n_i)$, obtained by the maximum-likelihood approach as well as the calibration method, and the experimental joint signal-idler photocount histogram $f_{si}(c_s,c_i)$ [see Fig. 2(a)] are plotted in Figs. 2(b) and 2(c), respectively. Thus, the analyzed twin beam contains tight (quantum) correlations between the signal and the idler photon numbers on one side, and on the other side its marginal signal and idler photon-number distributions are multithermal, i.e., very classical [16,46]. We note that the quantum properties of such weak noisy twin beams in multimode Gaussian states have been theoretically analyzed in Ref. [47] and the nonclassicality invariant describing the behavior of their entanglement on a beam splitter has been discussed in Refs. [48] and [49].

On the other hand, application of the maximum-likelihood approach provides a joint signal-idler photon-number distribution $p_{si}(n_s,n_i)$ as a steady state of the following iteration procedure [43,45]:

$$p_{si}^{(l+1)}(n_s,n_i) = p_{si}^{(l)}(n_s,n_i) \times \sum_{c_s,c_i} \frac{f_{si}(c_s,c_i)T_s(c_s,n_s)T_i(c_i,n_i)}{\sum_{n_s',n_i'} T_s(c_s,n_s')T_i(c_i,n_i')p_{si}^{(l)}(n_s',n_i')}, \quad l = 0,1,\ldots. \tag{101}$$

The uniform initial distribution $p_{si}^{(0)}(n_s,n_i)$ is assumed in the iteration procedure. Compared to the joint photon-number distribution p_{si} obtained in the calibration method, the distribution p_{si} revealed by the iteration procedure in Eq. (101) is broader, as documented in Fig. 2(b). This reflects slightly weaker correlations between the signal and the idler photon numbers (weaker pairing of photons), i.e., greater mean numbers of the noise signal and noise idler photons. As shown below, this is manifested when considering various entanglement criteria.

Nonclassicality (originating in local nonclassicality or entanglement) of a bipartite field is inscribed into its joint signal-idler quasidistribution $P_{si}(W_s,W_i)$ of integrated intensities W_s and W_i, which either attains negative values or does not exist as a regular analytical function [1,2]. In our case, we can obtain regularized forms of this quasidistribution either by direct

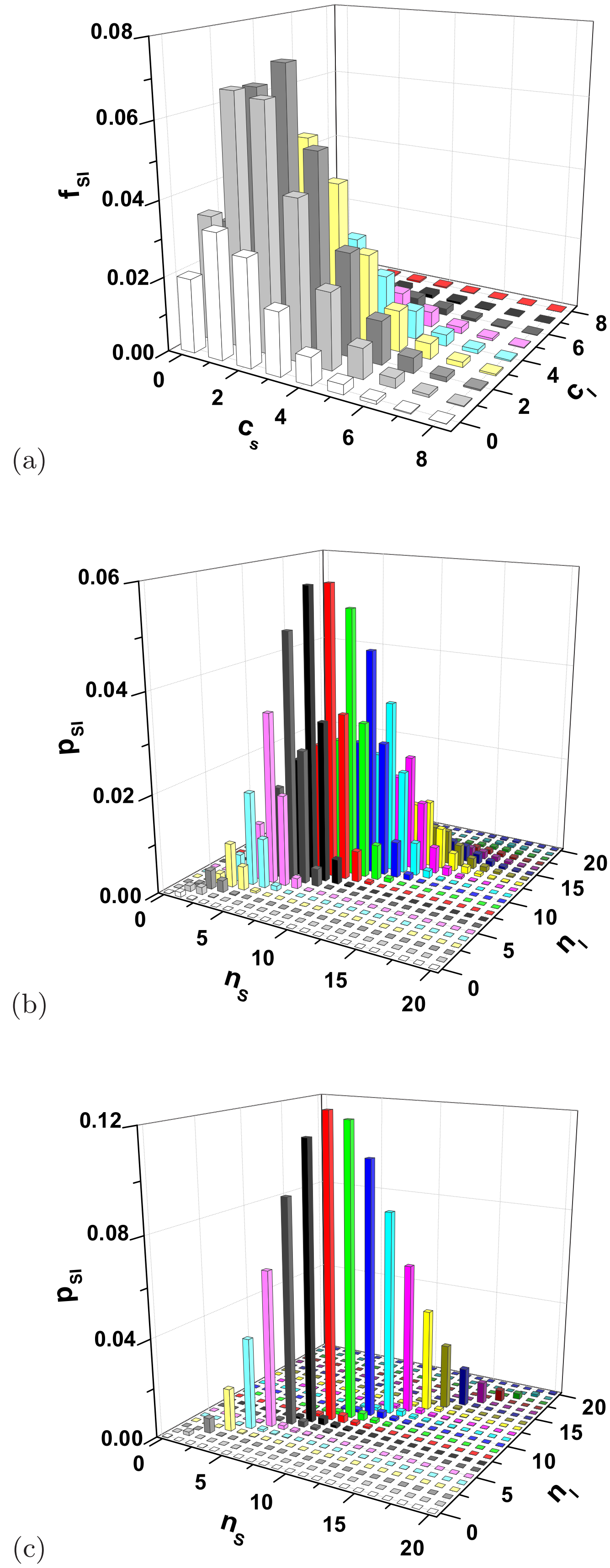

FIG. 2. (a) Experimental photocount histogram $f_{si}(c_s,c_i)$ and reconstructed photon-number distributions $p_{si}(n_s,n_i)$ obtained by (b) maximum-likelihood and (c) calibration methods.

evaluation (for a multimode Gaussian field) [25] or by use of the decomposition of the quasidistribution into specific series of Laguerre polynomials, with the weights derived from the appropriate joint photocount and photon-number distributions [16]. In both cases, regularization of the quasidistribution is provided by the experimental noise. Parallel strips with negative values are characteristic for the obtained regularized quasidistributions $P_{\rm si}(W_{\rm s},W_{\rm i})$, which are plotted in Fig. 3.

As the experimentally investigated noisy twin beams are mainly composed of photon pairs and exhibit multimode thermal photon-number statistics in both the signal and the idler fields, they cannot be locally nonclassical, but they exhibit entanglement. For this reason, we apply to the experimental histogram only the GNCCa derived in the previous two sections. We analyze both the joint experimental photocount histogram and the reconstructed joint photon-number distributions arising in the calibration and maximum-likelihood methods. We first pay attention to the GNCCa containing intensity moments. To allow for certain comparison among different GNCCa, we rewrite them in dimensionless units by introducing the normalized GNCCa (denoted by tildes). They are determined from the above written GNCCa by dividing them by appropriate powers of the mean intensity $\langle W\rangle = (\langle W_{\rm s}\rangle + \langle W_{\rm i}\rangle)/2$. However, fair comparison of the performance of various GNCCa containing intensity moments of different orders is based on the corresponding (global) NCDs τ introduced in Eq. (84). In the second step and for comparison, we analyze the GNCCa given in Eqs. (93)–(98), which use photon-number moments, and also some GNCCa involving the elements of photocount and photon-number distributions.

In our opinion, the GNCCa $E_{001},\ldots,E_{121}$ given in Eqs. (20)–(29) represent the basic set of GNCCa suggested for the analysis of entanglement restricted up to the fifth-order intensity moments. This is so because of their simple forms and the systematic inclusion of intensity moments of different orders. Moreover, they can be derived in parallel from the majorization theory and the inversion of simple classical inequalities valid for nonnegative polynomials. Also, the simplest GNCC written in Eq. (3) was experimentally measured already in 1991 [50]. The values of these GNCCa determined for the experimental photocount histogram (red stars), reconstructed photon-number distribution using the maximum-likelihood method (green triangles), and reconstructed photon-number distribution obtained by the calibration method (solid blue curve) are plotted in Fig. 4, together with the corresponding NCDs. Except for the GNCCa E_{301} and E_{031} applied to the photocount histogram, all other GNCCa from this basic set are negative, exhibiting entanglement. Positive values of the GNCCa E_{301} and E_{031} for the photocount histogram are related to the occurrence of the fifth-order marginal intensity moments in their definitions in Eqs. (26) and (27). Both types of the

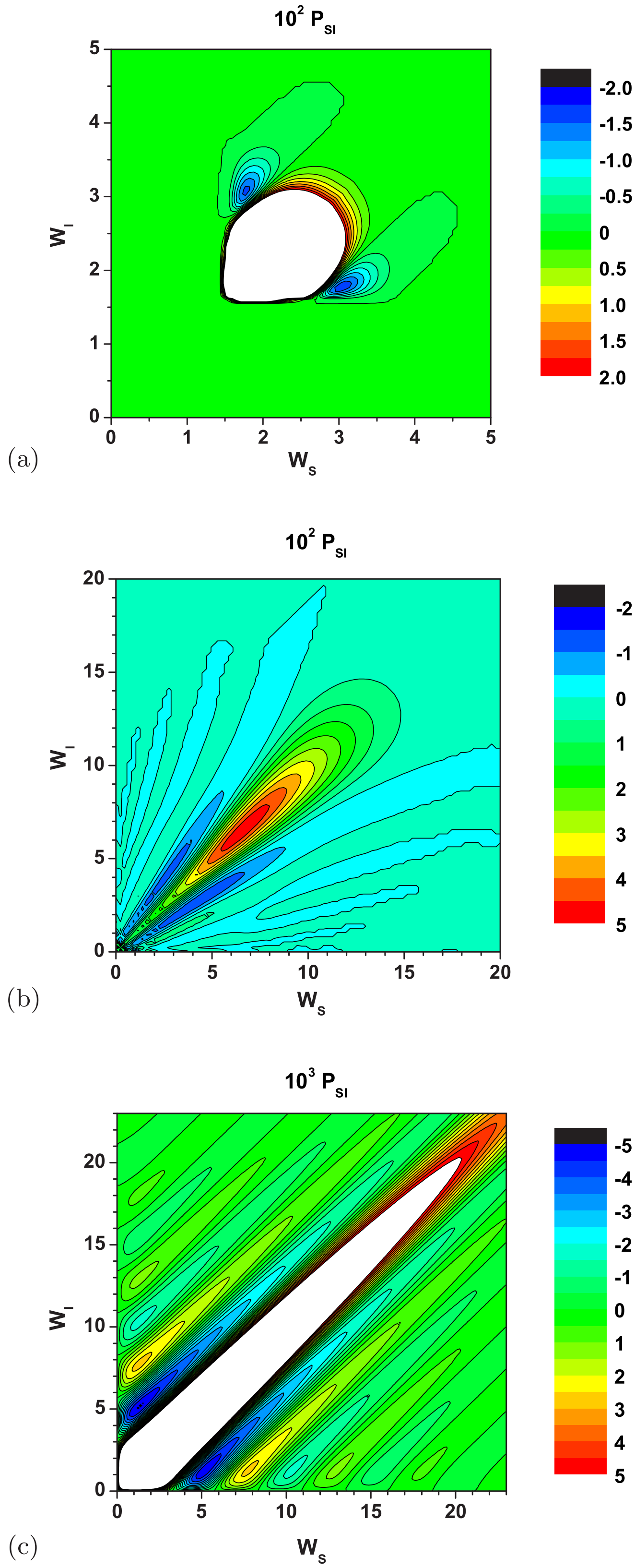

FIG. 3. Topo graphs of regularized quasidistributions $P_{\rm si}(W_{\rm s},W_{\rm i})$ of integrated intensities derived from (a) the experimental photocount histogram $f_{\rm si}$ (via its multi-mode Gaussian fit) for the ordering parameter $s=1$, (b) the photon-number distribution $p_{\rm si}$ reconstructed by the expectation-maximization approach (via the decomposition into Laguerre polynomials) for $s=0$, and (c) the photon-number distribution $p_{\rm si}$ reconstructed by the calibration method (via its multimode Gaussian fit) for $s=0.1$. In (a), the maximum of $P_{\rm si}$ within the white area equals 3.6×10^{-2}; in (c), 2.7×10^{-2}. When determining $P_{\rm si}$ in (a) and (c), one effective mode comprising the whole signal (idler) beam was assumed [3,16,21,25].

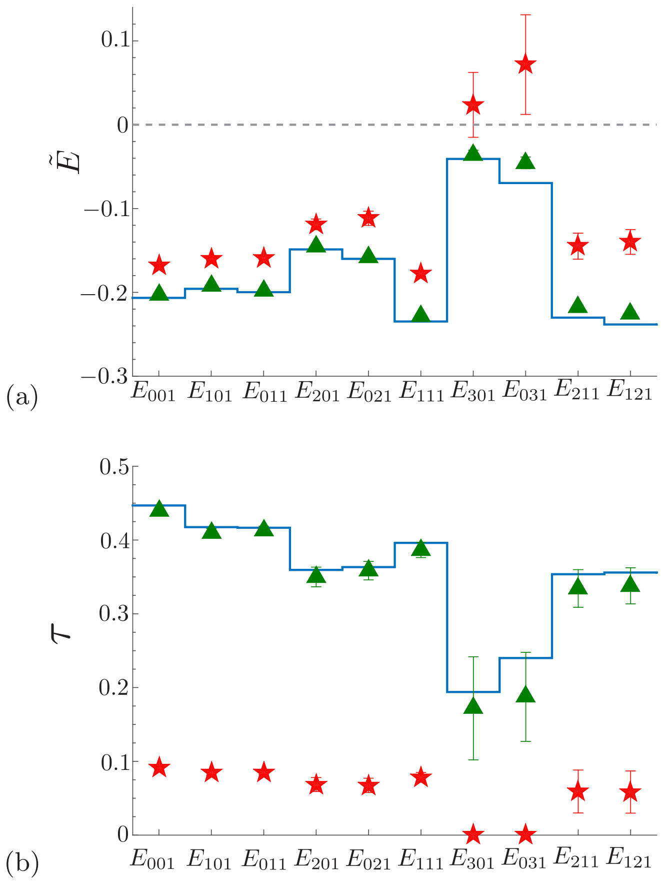

FIG. 4. (a) Normalized global nonclassicality criteria $\tilde{E}$ defined in Eqs (20)–(29) and (b) the corresponding nonclassicality depths τ. Values determined from the experimental photocount histogram are plotted with red stars; those appropriate for the reconstructed photon-number distribution reached by the maximum-likelihood (calibration) method by green triangles (solid blue curve). Some error bars are smaller than the symbols used.

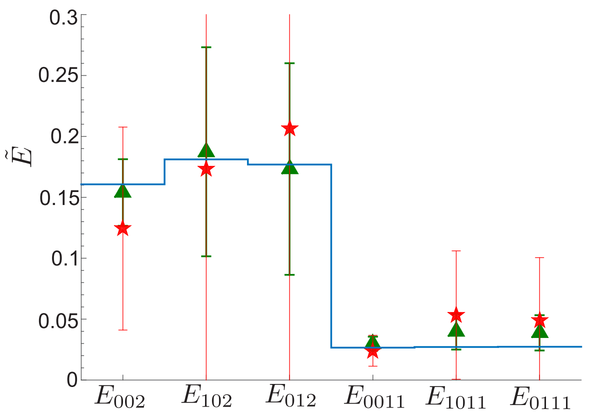

FIG. 5. Normalized global nonclassicality criteria $\tilde{E}$ defined in Eqs (30)–(32), (65), and (66). For description, see the caption to Fig. 4.

applied reconstructions that partly remove the noise from the detected photocount histogram lead to negative values of the GNCCa E_{301} and E_{031}. The analysis of the corresponding NCDs τ reveals that the values of NCDs τ decrease with increasing order of the intensity moments involved in the GNCCa. We note that a similar decrease in the values of NCDs with increasing order of intensity moments has been observed in [30] in the case of LNCCa. Naturally, the values of NCDs τ are considerably greater for the reconstructed photon-number distributions compared to the original experimental photocount histogram.

The basic set of GNCCa is accompanied by an additional six GNCCa that are derived similarly: E_{002} [Eq. (30)], E_{102} [Eq. (31)], E_{012} [Eq. (32)], E_{0011} [Eq. (66)], E_{1011} [Eq. (65)], and E_{0111}. Unfortunately, none of these GNCCa indicates entanglement in the measured twin beam, as documented in Fig. 5. Positive values of the GNCCa E_{002}, E_{102}, and E_{012} can again be related to the presence of the fourth- and fifth-order marginal intensity moments in the definitions of these GNCCa. On the other hand, the GNCCa E_{0011}, E_{1011}, and E_{0111} contain in their definitions terms with two and even three intensity moments in a product, which seriously limits their ability to reveal entanglement.

Restricting our consideration to fourth-order intensity moments, the majorization theory provides five GNCCa [denoted D; Eqs. (47)–(49)] for which products of two intensity moments are characteristic, together with nine GNCCa [denoted T; Eqs. (50)–(55)] containing terms with up to three intensity moments in a product. All these GNCCa indicate by their negative values entanglement in both the photocount histogram and the reconstructed photon-number distributions, as documented in Figs. 6 and 7. Mutual comparisons of NCDs τ for the GNCCa E, D, and T plotted in Figs. 4, 6, and 7, respectively, reveal that the entanglement described by the GNCCa E is the most resistant against noise, the GNCCa D are considerably worse from this point of view, and the resistance of the GNCCa T against noise is already weak. This behavior can qualitatively be explained by the occurrence of multiple products of intensity moments in the expressions giving the GNCCa D and T. These products do not naturally describe any correlation and so their presence in the GNCCa only weakens the ability of a given GNCCa to identify entanglement.

The widely used matrix approach [19,23,24] gives us three GNCCa, M_{1100} [Eq. (73)], M_{1001} [Eq. (74)], and M_{001001} [Eq. (77)], for investigating entanglement, provided that intensity moments up to the fifth order are taken into account.

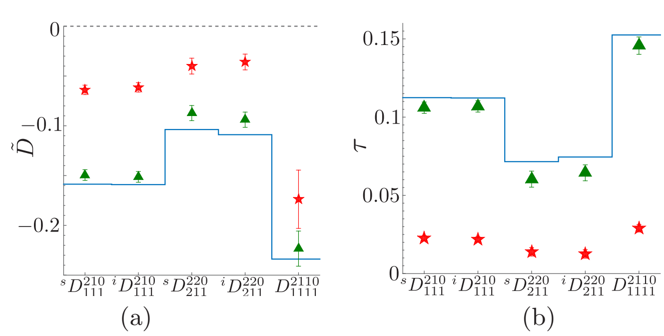

FIG. 6. (a) Normalized global nonclassicality criteria $\tilde{D}$ defined in Eqs (47)–(49) and (b) the corresponding nonclassicality depths τ. For description, see the caption to Fig. 4.

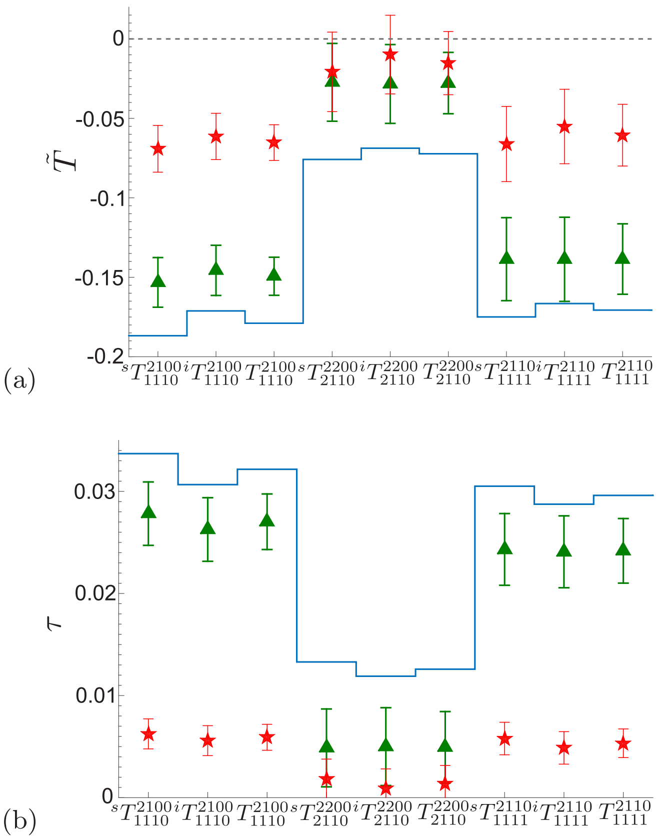

FIG. 7. (a) Normalized global nonclassicality criteria $\tilde{T}$ defined in Eqs (50)–(55) and (b) the corresponding nonclassicality depths τ. For description, see the caption to Fig. 4.

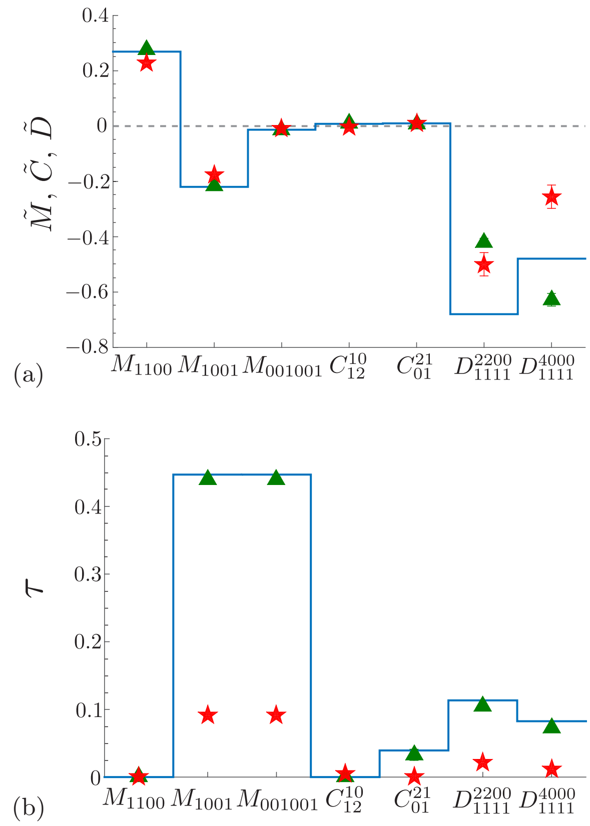

FIG. 8. (a) Normalized global nonclassicality criteria $\tilde{M}$, $\tilde{C}$, and $\tilde{D}$ defined in Eqs (73)–(77), (80), and (82) and (b) the corresponding nonclassicality depths τ. For description, see the caption to Fig. 4.

For our experimental data, only the GNCCa M_{1001} and M_{001001} identify entanglement (see Fig. 8). We note that negativity of the experimental GNCCa M_{1001} has been reported in [17]. The values of the corresponding NCDs τ plotted in Fig. 8 are comparable to those characterizing the GNCCa E from the basic set. This shows their high performance in identifying entanglement. A bit surprisingly, the GNCC M_{1100} is positive. In our opinion this is a consequence of the thermal statistics of photon pairs. Loosely speaking and relying on the quantum theory, we may define a 'photon-pair intensity' $W_{\rm si} \approx W_{\rm s} W_{\rm i}$, which allows us to rewrite Eq. (73) in the form $M_{1100} \approx \langle W_{\rm si}^2 \rangle - \langle W_{\rm si} \rangle^2$, explaining the positivity of the GNCC M_{1100} for the analyzed weak twin beam.

The Cauchy-Schwarz inequality provides two simple GNCCa not mentioned above, C_{12}^{10} [Eq. (80)] and C_{01}^{21} [Eq. (82)], whose performance in revealing entanglement lies between that of the GNCC M_{1001} and that of the GNCC M_{1100} (see Fig. 8). For the experimental twin beam, only the GNCC C_{01}^{21} applied to the reconstructed photon-number distributions indicates entanglement. As the GNCC C_{12}^{10} is derived from the GNCC C_{01}^{21} by substitution s $\leftrightarrow$ i, this demonstrates strong sensitivity of both GNCCa to the level of noise. The slightly lower mean of the signal noise photon number compared to that of the idler field (0.07 versus 0.15) is sufficient to observe the negative GNCC C_{01}^{21}. For comparison, we plot in Fig. 8 another two GNCCa, D_{1111}^{2200} [Eq. (75)] and D_{1111}^{4000} [Eq. (76)], which also contain the cross-correlation intensity moments $\langle W_{\rm s} W_{\rm i} \rangle$ and $\langle W_{\rm s}^2 W_{\rm i}^2 \rangle$ and are expressed as positive linear combinations of the already analyzed GNCCa. However, their NCDs τ are lower due to the additional terms with marginal higher-order intensity moments occurring in their definitions compared to the formulas for the GNCCa M written in Eqs. (74) and (77).

All the above discussed GNCCa, which are based on the intensity moments, can straightforwardly be converted into the corresponding GNCCa, which contain photocount and photon-number moments, using the linear relations between the two types of moments quantified by the Stirling numbers S [see Eq. (92)]. This is more or less formal for the reconstructed photon-number distributions. Contrary to this, such GNCCa are useful and convenient when experimental photocount histograms are analyzed. The reason is that these GNCCa can be applied directly to the experimental data. This is why we have suitably combined various GNCCa written for the intensity moments to arrive at a specific set of six simple GNCCa N written in Eqs. (93)–(98). All of them have been able to reveal entanglement in the experimental histogram, as documented in Fig. 9. However, we note that the GNCCa N are expressed as sums of intensity moments of different orders, and as such, their structure is less transparent compared to the original GNCCa based on the intensity moments.

The comparison of the results reached by the above discussed GNCCa applied to the photon-number distributions reconstructed by the maximum-likelihood approach and the

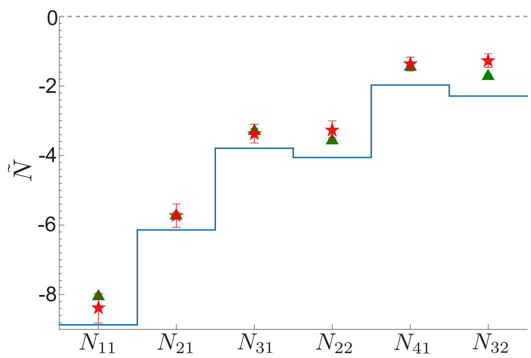

FIG. 9. Normalized global nonclassicality criteria $\tilde{N}$ defined in Eqs (93)–(98). For description, see the caption to Fig. 4. Normalization is done with respect to the corresponding quantities $N^{\rm ref}$ determined for the factorized distribution $P_{\rm s}(W_{\rm s})P_{\rm i}(W_{\rm i})$.

calibration method reveals the following. Negative values of the GNCCa, which reveal entanglement, reached by both approaches equal within the experimental errors or the values provided by the maximum-likelihood approach are greater than those reached by the calibration method. In consequence, the corresponding NCDs from both approaches coincide within the experimental errors or those arising in the calibration method are greater. This behavior naturally stems from the fact that the calibration method is more efficient in removing noise from the experimental data. This is so as the calibration method works with a predefined form of the photon-number distribution and applies it simultaneously to the whole two-dimensional experimental photocount histogram.

Finally, all the above written GNCCa as well as LNCCa can be transformed into the corresponding GNCCa and LNCCa, which involve the elements of photocount histogram or reconstructed photon-number distributions, using the formal substitution written in Eq. (89). The use of such GNCCa, however, requires an approach different from that applied to the GNCCa containing intensity moments. Whereas only intensity moments up to a certain order are useful, owing to the increasing experimental error with increasing order of the intensity moment, useful and reliable GNCCa in the case of the distributions involve their elements (probabilities) having the highest available values. As both the joint photocount histogram $f_{\rm si}$ and the joint reconstructed photon-number distributions $p_{\rm si}$ have such elements around the diagonal (see Fig. 2), we consider the GNCCa involving the elements at the diagonal [41,51] and the closest neighbor parallel lines, as described in turn by the functions F_{kk1}, $F_{(k+j)k1}$, and $F_{k(k+j)1}$, $j = 1,2$, with the varying index k (see Fig. 10). The GNCCa F defined in Eq. (90) reliably reveal entanglement via their negative values in the area around the peaks of both the photocount histogram ($k \approx 2$) and the reconstructed photon-number distributions ($k \approx 9$). We note that negative values of the GNCCa $F_{(k+j)k1}$ and $F_{k(k+j)1}$ for $j = 2,\ldots$ [$j = 1,\ldots$] have not been observed for the photon-number distribution reconstructed by the maximum-likelihood [calibration] method, which is a consequence of its narrow 'cigar' shape, clearly visible in Fig. 2(b) [2(c)].

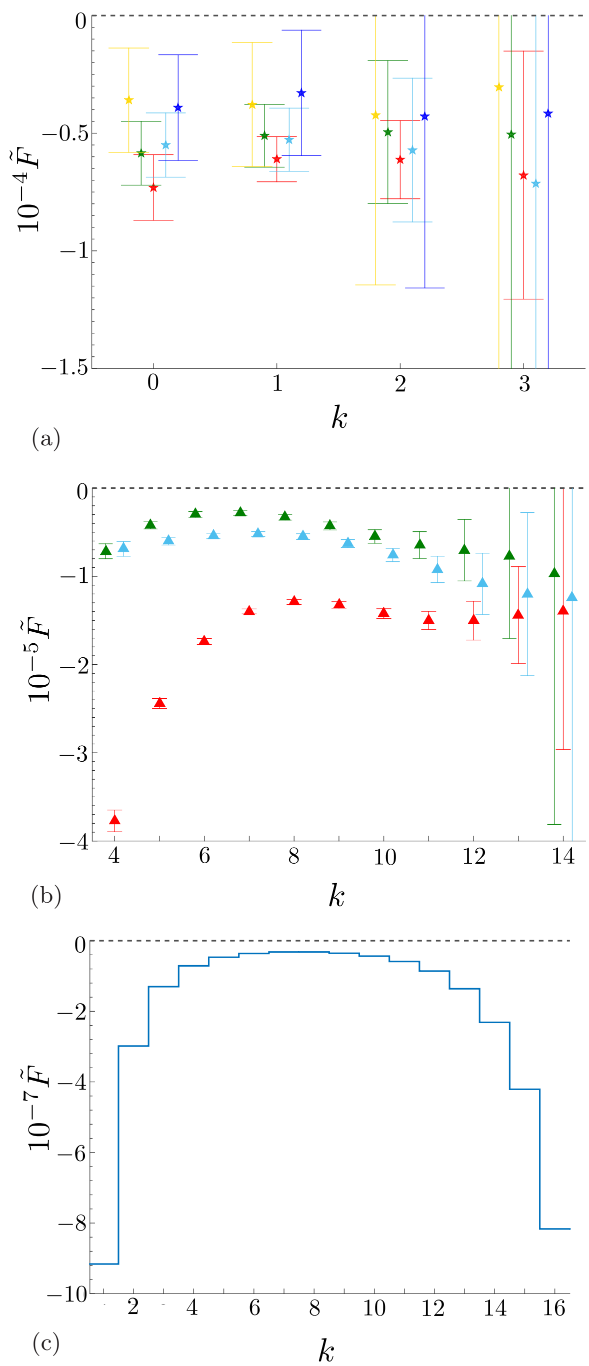

FIG. 10. Normalized global nonclassicality criterion $\tilde{F}_{k'l'1}$ given in Eq. (90) for (a) the experimental photocount histogram $f_{\rm si}$ and $k'l' = kk$ (red stars), $(k+1)k$ (green stars), $(k+2)k$ (yellow stars), $k(k+1)$ (light-blue stars), and $k(k+2)$ (dark-blue stars); (b) the photon-number distribution $p_{\rm si}$ reconstructed by the maximum-likelihood approach and $k'l' = kk$ (red triangles), $(k+1)k$ (green triangles), and $k(k+1)$ (blue triangles); and (c) the photon-number distribution $p_{\rm si}$ reconstructed by the calibration method for $k'l' = kk$ (solid blue curve), where $\tilde{F}_{kl1} \equiv [(k+1)(k+2)p_{\rm si}(k+2,l) + (l+1)(l+2)p_{\rm si}(k,l+2) - 2(k+1)(l+1)p_{\rm si}(k+1,l+1)]/[(k+1)(k+2)p_{\rm s}^{\rm P}(k+2)p_{\rm i}^{\rm P}(l) + (l+1)(l+2)p_{\rm s}^{\rm P}(k)p_{\rm i}^{\rm P}(l+2) - 2(k+1)(l+1)p_{\rm s}^{\rm P}(k+1)p_{\rm i}^{\rm P}(l+1)]$ and $p_a^{\rm P}(n)$ is the Poissonian distribution, with the mean $\langle n_a\rangle$ normalized such that $p_a^{\rm P}(0) = 1$, $a = {\rm s,i}$.

VI. CONCLUSIONS

We have derived numerous inequalities among the moments of integrated intensities aimed at identifying local as well as global nonclassicality using (a) the majorization theory, (b) nonnegative polynomials, (c) the matrix approach based on quadratic forms, and (d) the Cauchy-Schwarz inequality. We have mutually compared different approaches, grouped the obtained nonclassicality criteria according to their structure, and tested their performance on the experimental data characterizing a weak twin beam with about nine photon pairs per pulse and a small amount of additional noise. We have identified a basic set of 10 global nonclassicality criteria that reveal entanglement in the analyzed twin beam. We have also paid attention to the counterparts of the nonclassicality criteria written in the moments of photocounts and photon numbers and also the elements of photocount and photon-number distributions. We have demonstrated their performance on the same experimental data. For twin beams with a small amount of the noise all three kinds of nonclassicality criteria represent strong tools for revealing entanglement.

ACKNOWLEDGMENTS

The authors thank M. Hamar for his help with the experiment. The authors were supported by GA ČR (Project No. 15-08971S) and MŠMT ČR (Project No. LO1305). I.A. was supported by GA ČR (Project No. 17-23005Y) and UP (Project No. IGA_PrF_2017_005).

APPENDIX: ADDITIONAL (REDUNDANT) NONCLASSICALITY CRITERIA

In this Appendix, we summarize the nonclassicality criteria derived from the majorization theory with polynomials written in three and four variables and being redundant with respect to those presented in the text. This means that these LNCCa and GNCCa are expressed as positive linear combinations of the LNCCa and GNCCa reported in the text.

First, we summarize the redundant (and properly normalized) LNCCa that complement the LNCCa contained in Eqs. (35)–(40) and (56)–(59) ($a = \mathrm{s,i}$):

$$ {}^{a}B^{200}_{110} = {}^{a}L^{20}_{11} + B^{20}_{11} < 0, \tag{A1} $$

$$ {}^{a}B^{300}_{210} = {}^{a}L^{30}_{21} + B^{30}_{21} < 0, \tag{A2} $$

$$ {}^{a}B^{400}_{310} = {}^{a}L^{40}_{31} + B^{40}_{31} < 0, \tag{A3} $$

$$ {}^{a}B^{310}_{220} = {}^{a}L^{31}_{22} + B^{31}_{22} < 0, \tag{A4} $$

$$ {}^{a}B^{2000}_{1100} = 2\,{}^{a}L^{20}_{11} + B^{20}_{11} < 0, \tag{A5} $$

$$ B^{2000}_{1100} = {}^{\mathrm{s}}L^{20}_{11} +{}^{\mathrm{i}}L^{20}_{11} + 2B^{20}_{11} < 0, \tag{A6} $$

$$ {}^{a}B^{3000}_{2100} = 2^{a}L^{30}_{21} + B^{30}_{21} < 0, \tag{A7} $$

$$ B^{3000}_{2100} = {}^{\mathrm{s}}L^{30}_{21} +{}^{\mathrm{i}}L^{30}_{21} + 2B^{30}_{21} < 0, \tag{A8} $$

$$ {}^{a}B^{2100}_{1110} = \langle W_a\rangle\,{}^{a}L^{20}_{11} +{}^{a}B^{210}_{111} < 0, \tag{A9} $$

$$ B^{2100}_{1110} = {}^{\mathrm{s}}B^{210}_{111} +{}^{\mathrm{i}}B^{210}_{111} < 0, \tag{A10} $$

$$ {}^{a}B^{4000}_{3100} = 2\,{}^{a}L^{40}_{31} + B^{40}_{31} < 0, \tag{A11} $$

$$ B^{4000}_{3100} = {}^{\mathrm{s}}L^{40}_{31} +{}^{\mathrm{i}}L^{40}_{31} + 2B^{40}_{31} < 0, \tag{A12} $$

$$ {}^{a}B^{3100}_{2200} = 2\,{}^{a}L^{31}_{22} + B^{31}_{22} < 0, \tag{A13} $$

$$ B^{3100}_{2200} = {}^{\mathrm{s}}L^{31}_{22} +{}^{\mathrm{i}}L^{31}_{22} + 2B^{31}_{22} < 0, \tag{A14} $$

$$ {}^{a}B^{2200}_{2110} = \langle W_a^2\rangle\,{}^{a}L^{20}_{11} +{}^{a}B^{220}_{211} < 0, \tag{A15} $$

$$ B^{2200}_{2110} = {}^{\mathrm{s}}B^{220}_{211} +{}^{\mathrm{i}}B^{220}_{211} < 0. \tag{A16} $$

The redundant (and properly normalized) GNCCa containing terms with up to two intensity moments in a product attain the form ($a = \mathrm{s,i}$)

$$ {}^{a}D^{200}_{110} = {}^{a}L^{20}_{11} + \left(E_{001} + B^{20}_{11}\right)/2 < 0, \tag{A17} $$

$$ {}^{a}D^{300}_{210} = 2\,{}^{a}L^{30}_{21} + E_{101} + E_{011} + B^{30}_{21} < 0, \tag{A18} $$

$$ {}^{a}D^{400}_{310} = 2\,{}^{a}L^{40}_{31} + E_{201} + E_{111} + E_{021} + B^{40}_{31} < 0, \tag{A19} $$

$$ {}^{a}D^{310}_{220} = 2\,{}^{a}L^{31}_{22} + E_{111} + B^{31}_{22} < 0, \tag{A20} $$

$$ D^{2000}_{1100} = {}^{\mathrm{s}}L^{20}_{11} +{}^{\mathrm{i}}L^{20}_{11} + E_{001} + B^{20}_{11} < 0, \tag{A21} $$

$$ D^{3000}_{2100} = {}^{\mathrm{s}}L^{30}_{21} +{}^{\mathrm{i}}L^{30}_{21} + E_{101} + E_{011} + B^{30}_{21} < 0, \tag{A22} $$

$$ D^{2100}_{1110} = \left({}^{\mathrm{s}}D^{210}_{111} +{}^{\mathrm{i}}D^{210}_{111}\right)/2 < 0, \tag{A23} $$

$$ D^{4000}_{3100} = {}^{\mathrm{s}}L^{40}_{31} +{}^{\mathrm{i}}L^{40}_{31} + E_{201} + E_{111} + E_{021} + B^{40}_{31} < 0, \tag{A24} $$

$$ D^{3100}_{2200} = {}^{\mathrm{s}}L^{31}_{22} +{}^{\mathrm{i}}L^{31}_{22} + E_{111} + B^{31}_{22} < 0, \tag{A25} $$

$$ D^{2200}_{2110} = {}^{\mathrm{s}}D^{220}_{211} +{}^{\mathrm{i}}D^{220}_{211} < 0. \tag{A26} $$

Finally, the redundant (and properly normalized) GNCCa expressed via triple products of intensity moments are derived as follows ($a = \mathrm{s,i}$):

$$ {}^{a}T^{2000}_{1100} = 6\,{}^{a}L^{20}_{11} + E_{001} + 2B^{20}_{11} < 0, \tag{A27} $$

$$ T^{2000}_{1100} = {}^{\mathrm{s}}L^{20}_{11} +{}^{\mathrm{i}}L^{20}_{11} + \left(E_{001} + 3B^{20}_{11}\right)/2 < 0, \tag{A28} $$

$$ {}^{a}T^{3000}_{2100} = 6\,{}^{a}L^{30}_{21} + E_{101} + E_{011} + 2B^{30}_{21} < 0, \tag{A29} $$

$$ T^{3000}_{2100} = 2\,{}^{\mathrm{s}}L^{30}_{21} + 2\,{}^{\mathrm{i}}L^{30}_{21} + E_{101} + E_{011} + 3B^{30}_{21} < 0, \tag{A30} $$

$$ {}^{a}T^{4000}_{3100} = 6\,{}^{a}L^{40}_{31} + E_{201} + E_{111} + E_{021} + 2B^{40}_{31} < 0, \tag{A31} $$

$$ T^{4000}_{3100} = 2\,{}^{\mathrm{s}}L^{40}_{31} + 2\,{}^{\mathrm{i}}L^{40}_{31} + E_{201} + E_{111} + E_{021} + 3B^{40}_{31} < 0, \tag{A32} $$

$$ {}^{a}T^{3100}_{2200} = 6\,{}^{a}L^{31}_{22} + E_{111} + 2B^{31}_{22} < 0, \tag{A33} $$

$$ T^{3100}_{2200} = 2\,{}^{\mathrm{s}}L^{31}_{22} + 2\,{}^{\mathrm{i}}L^{31}_{22} + E_{111} + 3B^{31}_{22} < 0. \tag{A34} $$

[1] R. J. Glauber, Coherent and incoherent states of the radiation field, Phys. Rev. **131**, 2766 (1963).
[2] E. C. G. Sudarshan, Equivalence of Semiclassical and Quantum Mechanical Descriptions of Statistical Light Beams, Phys. Rev. Lett. **10**, 277 (1963).
[3] J. Peřina, *Quantum Statistics of Linear and Nonlinear Optical Phenomena* (Kluwer, Dordrecht, Netherlands, 1991).
[4] L. Mandel and E. Wolf, *Optical Coherence and Quantum Optics* (Cambridge University Press, Cambridge, UK 1995).
[5] W. Vogel, D. G. Welsch, and S. Walentowicz, *Quantum Optics* (Wiley-VCH, Weinheim, 2001).
[6] V. V. Dodonov and V. I. Man'ko, Nonclassical states in quantum physics: Brief historical review, in, editors, *Theory of Nonclassical States of Light*, edited by V. V. Dodonov and V. I. Man'ko (Taylor and Francis, London, 2003), pp. 1–80.
[7] M. V. Fedorov and M. I. Miklin, Schmidt modes and entanglement, Contemp. Phys. **55**, 94 (2014).
[8] A. Kenfack and K. Zyczkowski, Negativity of the Wigner function as an indicator of non-classicality, J. Opt. B **6**, 396 (2004).
[9] K. W. Chan, J. P. Torres, and J. H. Eberly, Transverse entanglement migration in Hilbert space, Phys. Rev. A **75**, 050101(R) (2007).
[10] F. Just, A. Cavanna, M. V. Chekhova, and G. Leuchs, Transverse entanglement of biphotons, New J. Phys. **15**, 083015 (2013).
[11] U. Leonhardt, *Measuring the Quantum State of Light* (Cambridge University Press, Cambridge, UK, 1997).
[12] A. I. Lvovsky and M. G. Raymer, Continuous-variable optical quantum state tomography, Rev. Mod. Phys. **81**, 299 (2009).
[13] A. Peres, Separability Criterion for Density Matrice, Phys. Rev. Lett. **77**, 1413 (1996).
[14] M. Horodecki, P. Horodecki, and R. Horodecki, Separability of mixed states: Necessary and sufficient conditions, Phys. Lett. A **223**, 1 (1996).
[15] S. Hill and W. K. Wootters, Computable Entanglement, Phys. Rev. Lett. **78**, 5022 (1997).
[16] O. Haderka, J. Peřina, Jr., M. Hamar, and J. Peřina, Direct measurement and reconstruction of nonclassical features of twin beams generated in spontaneous parametric down-conversion, Phys. Rev. A **71**, 033815 (2005).
[17] A. Allevi, S. Olivates, and M. Bondani, Measuring high-order photon-number correlations in experiments with multimode pulsed quantum states, Phys. Rev. A **85**, 063835 (2012).
[18] A. Allevi, M. Lamperti, M. Bondani, J. Peřina, Jr., V. Michálek, O. Haderka, and R. Machulka, Characterizing the nonclassicality of mesoscopic optical twin-beam states, Phys. Rev. A **88**, 063807 (2013).
[19] J. Sperling, M. Bohmann, W. Vogel, G. Harder, B. Brecht, V. Ansari, and C. Silberhorn, Uncovering Quantum Correlations with Time-Multiplexed Click Detection, Phys. Rev. Lett. **115**, 023601 (2015).
[20] G. Harder, T. J. Bartley, A. E. Lita, S. W. Nam, T. Gerrits, and C. Silberhorn, Single-Mode Parametric-Down-Conversion States with 50 Photons as a Source for Mesoscopic Quantum Optics, Phys. Rev. Lett. **116**, 143601 (2016).
[21] J. Peřina, Jr., O. Haderka, V. Michálek, and M. Hamar, State reconstruction of a multimode twin beam using photodetection, Phys. Rev. A **87**, 022108 (2013).
[22] A. W. Marshall, I. Olkin, and B. C. Arnold, *Inequalities: Theory of Majorization and Its Application*, 2nd ed. (Springer, New York, 2010).
[23] W. Vogel, Nonclassical Correlation Properties of Radiation Fields, Phys. Rev. Lett. **100**, 013605 (2008).
[24] A. Miranowicz, M. Bartkowiak, X. Wang, X.-Y. Liu, and F. Nori, Testing nonclassicality in multimode fields: A unified derivation of classical inequalities, Phys. Rev. A **82**, 013824 (2010).
[25] J. Peřina and J. Křepelka, Multimode description of spontaneous parametric down-conversion, J. Opt. B **7**, 246 (2005).
[26] C. T. Lee, General criteria for nonclassical photon statistics in multimode radiations, Opt. Lett. **15**, 1386 (1990).
[27] C. T. Lee, Higher-order criteria for nonclassical effects in photon statistics, Phys. Rev. A **41**, 1721 (1990).
[28] A. Verma and A. Pathak, Generalized structure of higher order nonclassicality, Phys. Lett. A **374**, 1009 (2010).
[29] I. I. Arkhipov, J. Peřina, Jr., V. Michálek, and O. Haderka, Experimental detection of nonclassicality of single-mode fields via intensity moments, Opt. Express **24**, 29496 (2016).
[30] J. Peřina, Jr., V. Michálek, and O. Haderka, Higher-order sub-Poissonian-like nonclassical fields: Theoretical and experimental comparison, Phys. Rev. A **96**, 033852 (2017).
[31] H. J. Kimble, M. Dagenais, and L. Mandel, Photon Antibunching in Resonance Fluorescence, Phys. Rev. Lett. **39**, 691 (1977).
[32] G. Agarwal and K. Tara, Nonclassical character of states exhibiting no squeezing or sub-Poissonian statistics, Phys. Rev. A **46**, 485 (1992).
[33] E. Shchukin, T. Richter, and W. Vogel, Nonclassicality criteria in terms of moments, Phys. Rev. A **71**, 011802(R) (2005).
[34] E. Shchukin and W. Vogel, Inseparability Criteria for Continuous Bipartite Quantum States, Phys. Rev. Lett. **95**, 230502 (2005); A. Miranowicz and M. Piani, Comment on "Inseparability Criteria for Continuous Bipartite Quantum States," *ibid.* **97**, 058901 (2006).
[35] T. Richter and W. Vogel, Nonclassicality of Quantum States: A Hierarchy of Observable Conditions, Phys. Rev. Lett. **89**, 283601 (2002).
[36] S. Ryl, J. Sperling, E. Agudelo, M. Mraz, S. Köhnke, B. Hage, and W. Vogel, Unified nonclassicality criteria, Phys. Rev. A **92**, 011801(R) (2015).
[37] I. S. Gradshtein and I. M. Ryzhik, *Table of Integrals, Series, and Products*, 6th ed. (Academic Press, San Diego, CA, 2000).
[38] C. T. Lee, Measure of the nonclassicality of nonclassical states, Phys. Rev. A **44**, 2775(R) (1991).
[39] D. N. Klyshko, Observable signs of nonclassical light, Phys. Lett. A **213**, 7 (1996).
[40] E. Waks, E. Diamanti, B. C. Sanders, S. D. Bartlett, and Y. Yamamoto, Direct Observation of Nonclassical Photon Statistics in Parametric Down-Conversion, Phys. Rev. Lett. **92**, 113602 (2004).
[41] E. Waks, B. C. Sanders, E. Diamanti, and Y. Yamamoto, Highly nonclassical photon statistics in parametric down-conversion, Phys. Rev. A **73**, 033814 (2006).
[42] A. Allevi, S. Olivates, and M. Bondani, High-order photon-number correlations: A resource for characterization and applications of quantum states, Int. J. Quantum. Info. **10**, 1241003 (2012).

[43] J. Peřina, Jr., M. Hamar, V. Michálek, and O. Haderka, Photon-number distributions of twin beams generated in spontaneous parametric down-conversion and measured by an intensified CCD camera, Phys. Rev. A **85**, 023816 (2012).

[44] J. Peřina, Jr., O. Haderka, M. Hamar, and V. Michálek, Absolute detector calibration using twin beams, Opt. Lett. **37**, 2475 (2012).

[45] A. P. Dempster, N. M. Laird, and D. B. Rubin, Maximum likelihood from incomplete data via the EM algorithm, J. R. Stat. Soc. B **39**, 1 (1977).

[46] M. Avenhaus, K. Laiho, M. V. Chekhova, and C. Silberhorn, Accessing Higher-Order Correlations in Quantum Optical States by Time Multiplexing, Phys. Rev. Lett. **104**, 063602 (2010).

[47] I. I. Arkhipov, J. Peřina, Jr., J. Peřina, and A. Miranowicz, Comparative study of nonclassicality, entanglement, and dimensionality of multimode noisy twin beams, Phys. Rev. A **91**, 033837 (2015).

[48] I. I. Arkhipov, J. Peřina, Jr., J. Peřina, and A. Miranowicz, Interplay of nonclassicality and entanglement of two-mode Gaussian fields generated in optical parametric processes, Phys. Rev. A **94**, 013807 (2016).

[49] I. I. Arkhipov, J. Peřina, Jr., J. Svozilík, and A. Miranowicz, Nonclassicality invariant of general two-mode Gaussian states, Sci. Rep. **6**, 26523 (2016).

[50] X. Y. Zou, L. J. Wang, and L. Mandely, Violation of classical probability in parametric down-conversion, Opt. Commun. **84**, 351 (1991).

[51] C. T. Lee, Simple criterion for nonclassical two-mode states, J. Opt. Soc. Am. B **15**, 1187 (1998).